Geophys. J. Int. (2004) **159,** 417–434 doi: 10.1111/j.1365-246X.2004.02402.x

Variations in the Earth's gravity field caused by torsional oscillations in the core

Mathieu Dumberry and Jeremy Bloxham

Department of Earth and Planetary Sciences, Harvard University, 20 Oxford Street, Cambridge, MA, 02138, *USA.*
E-mail: dumberry@mail.geophysics.harvard.edu

Accepted 2004 June 29. Received 2004 June 23; in original form 2003 November 17

SUMMARY

We investigate whether a component of the flow in the Earth's fluid core, namely torsional oscillations, could be detected in gravity field data at the surface and whether it could explain some of the observed time variations in the elliptical part of the gravity field (J_2). Torsional oscillations are azimuthal oscillations of rigid coaxial cylindrical surfaces and have typical periods of decades. This type of fluid motion supports geostrophic pressure gradients, which produce deformations of the core–mantle boundary. Because of the density discontinuity between the core and the mantle, such deformations produce changes in the gravity field that, because of the flow geometry, are both axisymmetric and symmetric about the equator. Torsional oscillations are thus expected to produce time variations in the zonal harmonics of even degree in the gravity field. Similarly, the changes in the rotation rates of the mantle and inner core that occur to balance the change in angular momentum carried by the torsional oscillations also produce zonal variations in gravity. We have built a model to calculate the changes in the gravity field and in the rotation rates of the mantle and inner core produced by torsional oscillations. We show that the changes in the rotation rate of the inner core produce changes in J_2 that are a few orders of magnitude too small to be observed. The amplitudes of the changes in J_2 from torsional oscillations are 10 times smaller than the temporal changes that are observed to occur about a linear secular trend. However, provided the mechanism responsible for these changes in J_2 is identified and that this contribution is removed from the data, it may be possible in the future to detect the lowest harmonic degrees of the torsional oscillations in the gravity field data. We also show that torsional oscillations have contributed to the linear secular change in J_2 by about -0.75×10^{-12} per year in the last 20 years. Finally, the associated change in the vertical ground motion at the surface of the Earth that is predicted by our mechanism is of the order of 0.2 mm, which is too small to be detected with the current precision in measurements.

Key words: core–mantle boundary, Earth's core, Earth's rotation, figure of Earth, gravity field, torsional oscillations.

1 INTRODUCTION

Torsional oscillations are the azimuthal oscillations of rigid cylindrical surfaces aligned with the rotation axis (Taylor 1963; Braginsky 1970) (Fig. 1). This type of flow is predicted to occur in the core as a result of Taylor's constraint (Taylor 1963), which specifies that, in steady state, the axial torque exerted by the magnetic force on any such cylindrical surface must vanish. If at any time this constraint is not satisfied on one cylindrical surface, a rigid azimuthal acceleration of the whole cylindrical surface is instigated in order to balance the torque. This process excites torsional oscillations, which have typical periods of a few decades and shorter (Braginsky 1970, 1984).

Because of their rigid nature, it is possible to retrieve the torsional oscillations from flow maps at the core–mantle boundary (CMB): one can simply take the part of the axisymmetric azimuthal velocity that is symmetric about the equator (Jault *et al.* 1988; Jackson *et al.* 1993; Zatman & Bloxham 1997; Hide *et al.* 2000; Pais & Hulot 2000). The torsional oscillations computed in this manner can be tested against an independent data set: since angular momentum of the whole Earth has to be conserved, the variations in time of the core angular momentum carried by torsional oscillations must be consistent with the changes in angular momentum of the mantle that are observed in terms of variations in its rotation rate (i.e. length-of-day variations). The agreement is especially good for the last few decades (Jault *et al.* 1988; Jackson *et al.* 1993),

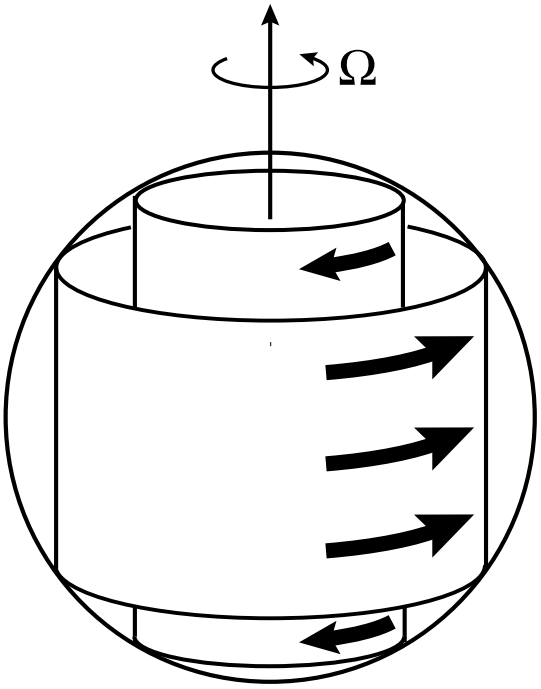

Figure 1. Torsional oscillations in the core.

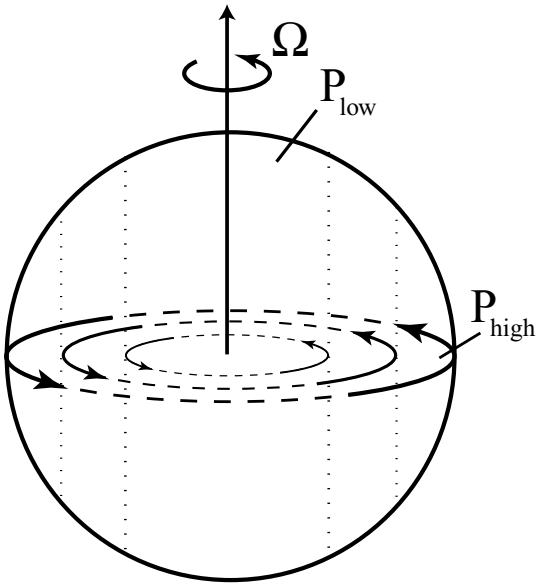

Figure 2. A prograde rigid rotation flow in the core (black arrows) gives rise to a geostrophic pressure that increases (quadratically) with distance from the rotation axis (Ω), from a low at the rotation axis to a high near the equator on the CMB. The flow and pressure are invariant in the direction parallel to the rotation axis.

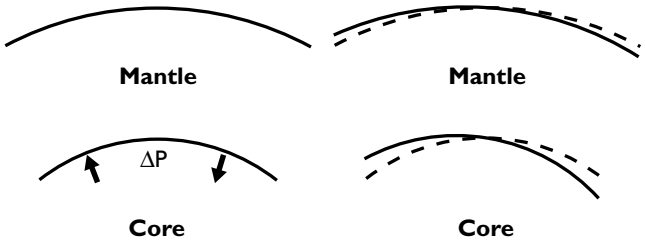

Figure 3. Horizontal gradients in pressure at the CMB (left) lead to a radial deformation of the CMB and the exterior surface (right).

which places a high degree of confidence on the retrieved torsional oscillations.

Since it is the only component of the flow inside the core that we know with confidence, torsional oscillations are the window through which we can observe several aspects of the dynamics of the core. For instance, the restoring force that maintains the oscillations depends on the strength of the magnetic field perpendicular to the cylindrical surfaces, and therefore by investigating the periodicity and radial structure of the oscillations it is possible to extract information about the magnetic field inside the core (Zatman & Bloxham 1997, 1998). Likewise, the attenuation of the waves contains information about the nature of the coupling between the core and the mantle at the CMB (Buffett 1998; Zatman & Bloxham 1999; Mound & Buffett 2003). In addition, constraints about the dynamics involved in the convective motions in the Earth's core may be inferred from the requirement that these dynamics be able to excite and maintain torsional oscillations (Dumberry & Bloxham 2003).

Recently, it has been shown that, although there remains some unexplained signal, a large part of the secular variation of the geomagnetic field, including the 'geomagnetic jerks', can be explained by a steady flow plus a more refined model of torsional oscillations (Bloxham *et al.* 2002). More accurate models of torsional oscillations, in the spirit of this latter study, can then lead to a better characterization of some of the core processes. The current models are obtained by inverting the flows at the CMB capable of explaining the secular variation of the geomagnetic field. Torsional oscillations may also be constrained to be consistent with length-of-day variations. In this study, we propose a new way to attempt to observe, and therefore provide additional constraints on, torsional oscillations. We investigate whether it is possible to detect them in the gravity field data at the surface of the Earth.

The large Coriolis force associated with rigid azimuthal flows of the sort involved in torsional oscillations is balanced by the establishment of a pressure gradient in the direction perpendicular to the rotation axis. This geostrophic force balance provides a simple way to visualize how torsional oscillations produce variations in the gravity field. Consider for example a prograde rigid rotation of the whole core, where the rigid azimuthal velocity increases linearly with distance from the rotation axis (Fig. 2). This requires the establishment of a low pressure along the rotation axis and a high pressure at the equator of the CMB, with surfaces of constant pressure coinciding with surfaces of coaxial cylinders. This geostrophic pressure gradient from the pole to the equator along the CMB produces latitudinal variations in surface forces on the CMB and deformations of this fluid–solid surface. The distortion of the CMB produces variations in the gravity field because there exists a large density discontinuity between the core and the mantle. The perturbation in gravity leads to adjustments in the mechanical equilibrium of the whole planet. It may then be observed at the surface, although with attenuated amplitude (Fig. 3). A similar effect is produced at the inner core boundary (ICB), with radial displacements of this boundary contributing to variations in the global gravity field. However, because the density discontinuity between the inner core and the fluid core is smaller, and because it is further away from the surface, we expect the contribution at the ICB to be less important than that at the CMB.

An additional effect that needs to be considered is the gravity field perturbation that results from the changes in the rotation rate

of the mantle. As we have already mentioned, these are required in order to balance the changes in the axial angular momentum of the core carried by torsional oscillations. Changes in the rotation rate of the mantle modify the equilibrium balance between gravity and centrifugal forces. Consequently, this changes the elliptical component of the gravity field and the oblateness of the Earth. The change in the gravity field produced by the latter effect is opposite to the direct effect of the pressure force on the CMB produced by the torsional oscillations. So, for instance, if torsional oscillations produce a prograde net rotation of the core and tend to make the whole Earth more oblate, the associated retrograde rotation of the mantle tends to make the Earth less oblate.

A similar effect arises from changes in the rotation rate of the inner core. Because of strong electromagnetic coupling at the ICB (Gubbins 1981), torsional oscillations will cause the inner core to undergo changes in its rotation rate. In addition, because of axial gravitational coupling between the mantle and the inner core (Buffett 1996), a change in the rotation rate of one influences the other. As for the mantle, changes in the rotation rate of the inner core produce changes in oblateness and in the elliptical gravity field of the whole Earth.

Torsional oscillations are time-dependent flows, and because of their geometry we expect them to produce variations in the zonal harmonics of even degree in the gravity field. Hence, it may possible to detect time variations in the zonal components of the gravity field that are caused by the torsional oscillations. If so, the gravity data may then be used to provide better constraints on models of torsional oscillations.

An additional motivation for this investigation comes from the gravity field data themselves. Large subdecadal timescale changes in the degree 2 zonal harmonic of the gravitational field have recently been reported (Cox & Chao 2002), and these may perhaps be caused by the dynamical mechanism proposed above. As shown in Fig. 4, prior to 1998 the variations in the coefficient J_2, which represents a measure of the degree 2 zonal harmonic (e.g. Jeffreys 1970), seem to consist essentially of a slowly decreasing linear drift of $\sim -2.8 \times 10^{-11}$ yr^{-1}. This linear secular trend is thought to represent the signature of postglacial rebound: polar land masses are still uplifting from the removal of the glacier load that covered them during the last glaciation, resulting in a gradually less oblate Earth (Yoder *et al.* 1983; Rubincam 1984; Mitrovica & Peltier 1993), and hence a decrease in J_2. However, a considerable departure from this linear trend has occurred between 1998 and 2002. This impulse in the signal is difficult to reconcile with the slow process of postglacial rebound for which the timescale of variations is about a thousand years. Therefore this suggests the presence of at least one additional physical mechanism that participates in the temporal changes of J_2. Moreover, the fact that ΔJ_2 is now on its way back to its pre-1998 trend suggests that this additional mechanism may be episodic and does not produce permanent changes.

The sudden increase in J_2 requires a mass transport from the polar regions to the equatorial regions, or an increase in the oblateness of the whole Earth, or a combination of both. In the original report of the impulse, Cox & Chao (2002) suggested possible mechanisms involving mass transport in the oceans and the atmosphere, and glacier-melting near the polar regions, although none of these possibilities was shown to be entirely satisfactory. More recently, Chao *et al.* (2003) have shown that variations in sea-surface height in the extratropic north and south Pacific ocean basins have a combined temporal variation that matches remarkably well the time evolution of the recent sudden changes in J_2. However, the amplitude of the variations predicted from this oceanographic event accounts for only one-third of the observed anomaly. It has been proposed that the remaining part of the signal can be explained by glacier-melting at subpolar latitudes (Dickey *et al.* 2002). However, the sea-level rise that would accompany the ice-melt has not been observed (Chao *et al.* 2003), which suggests that the melt water, if any, remained in the vicinity of its melting location, in which case there is no transport of mass towards the equator and no associated increase in J_2. Another problem with the latter scenario is that it should produce a sizable anomaly in J_3, which is not observed (Chao *et al.* 2003). In addition, it is difficult to explain the return of J_2 to its pre-1998 trend with a glacier-melting mechanism, because it would imply the reverse scenario: a sudden large accumulation of ice and snow at high latitude and a consistent sea-level drop, neither of which has been observed. Since it is more likely that the departures in J_2 are caused by a single mechanism, this raises doubts on the validity of the glacier-melting scenario.

Another possibility suggested by Cox & Chao (2002) involves the Earth's fluid core. As they pointed out, a geomagnetic jerk occurred in 1999 (Mandea *et al.* 2000), in proximity to the time at which the departure in J_2 was recorded. Geomagnetic jerks, as we have mentioned above, can be explained by torsional oscillations in the core (Bloxham *et al.* 2002). This indicates a possible correlation between the changes in J_2 and torsional oscillations. Moreover, geomagnetic jerks have also been observed in 1978 (Gavoret *et al.* 1986; Gubbins & Tomlinson 1986) and 1991 (Macmillan 1996), and near both of these times we observe a somewhat larger departure of J_2 from the linear trend. These correlations suggest that jerks and changes in J_2 may have a common explanation and call for a

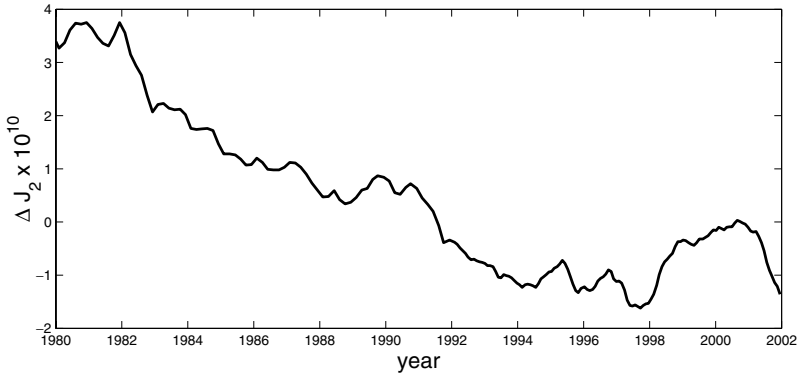

Figure 4. Variations in time of J_2 from satellite laser ranging data, once the seasonal contributions are subtracted. The data presented are those obtained after a filtering by a 1-yr moving window (adapted from Cox & Chao 2002).

proper investigation of the contribution of torsional oscillations in the gravity field data.

In order to do this, we have built a model that predicts the variations in the gravitational potential caused by a given torsional oscillation flow model. This model computes the displacements, the changes in the gravity field and the changes in the stress field in the entire Earth that are produced by the radial forcing associated with torsional oscillations and changes in rotation rates of the mantle and inner core. We find that, by using a torsional oscillation flow model that is constrained to satisfy the length-of-day data and also provide the best fit to the geomagnetic jerk signals, the changes in J_2 that are predicted by our model are not well correlated with the observed changes, and have a magnitude 10 times too small. This suggests that the sudden observed changes in J_2 cannot be explained directly by torsional oscillations and that the correlation between the geomagnetic jerks and the maxima in ΔJ_2 may be a coincidence. However, provided the origin of these large variations is identified and removed from the data, it may be possible in the future to detect torsional oscillations in the gravity field data. We note that only the lowest harmonics of torsional oscillations, t_1^0 and t_3^0, may produce changes in gravity large enough to be observed. Our model also predicts the occurrence of vertical ground motions of the order of 0.2 mm, which is presently too small to be observed, but may be observable in the near future. The results of our model also suggest that torsional oscillations have contributed to a secular change in J_2 of about -0.75×10^{-12} per year in the last 20 yr. In addition, our results indicate that the changes in the rotation rate of the inner core induced by torsional oscillations or other means produce variations in J_2 that are a few orders of magnitude too small to be observed.

Finally, we note that the two main physical concepts dealt with in the present work have been discussed in previous studies. First, the idea that changes in the gravity field at the surface could be caused by pressure changes due to flow in the core which produce deflections of the CMB has been investigated most recently in the work of Fang *et al.* (1996). In their work, the change in geostrophic pressure at the CMB was deduced from the changes in the CMB flow between 1965 and 1975. This pressure field was then treated as a surface mass density perturbation at the CMB and the radial deflection and changes in the gravity field that resulted solely from this local perturbation were calculated. They reported changes in J_2 of the order of 1.3×10^{-11} per year, similar in amplitudes to the observed changes reported by Cox & Chao (2002) and larger by about an order of magnitude than the results of the present study. This large discrepancy is partly due to differences in modelling. We specify the geostrophic pressure in terms of a surface force acting on the CMB instead of a surface mass density perturbation. In addition, we solve for the resulting perturbations in the whole planet, instead of in the mantle only. The earlier work of Lefftz & Legros (1992) is also noteworthy, showing that variations in the topography at the CMB, for instance due to mantle convection, can produce significant changes in the gravity field. Secondly, the changes in the elliptical component of the gravity field resulting from variations in rotation rate of the mantle (and inner core) is also not a novel idea. Indeed, the discrepancy between the observed and predicted values of the hydrostatic flattening was erroneously believed for a long time to be related to the deceleration of the Earth's rotation rate (e.g. Munk & MacDonald 1960). More recently, Denis *et al.* (1998) have calculated the changes in elliptical gravity field that result from changes in rotation rate, and the method employed in the present work is inspired in many ways from this study. We note that the inclusion of this effect in our calculation is also responsible for part of the difference from the results of Fang *et al.* (1996).

2 THEORY

We seek to determine the displacements and changes in the gravity field and stress field of the whole Earth that result from specified forcings: torsional oscillations in the fluid core and rotation rate changes in the mantle and inner core. The dynamics governing small perturbations in the mechanical equilibrium of a self-gravitating Earth is a well-studied problem because it lies at the very base of the theoretical foundation on which normal-mode seismology is built. In addition, the responses of the Earth to external forcing, such as tidal forcing, and to surface loading, such as postglacial rebound and sea-level change, are also based on the same theoretical framework. We take advantage of this extensive body of literature to construct our model.

The following assumptions and approximations are used. We assume that the undeformed Earth is spherically symmetric, self-gravitating and in hydrostatic equilibrium and consider the perturbations about that state. The spherically symmetric equilibrium implies that we are considering a reference state that is non-rotating. We also assume that the rotation does not influence the deformations in the sense that we neglect their associated Coriolis acceleration. The influence of rotation only enters our system through our prescription of the forcing in the fluid core, the inner core and the mantle that perturb the undeformed state. We are considering the static response due to static forcings and we assume that a static equilibrium is maintained at all times during the deformations. In other words, we neglect all inertial accelerations in the momentum balance. We assume that the fluid core is inviscid and remains in hydrostatic equilibrium even in the deformed state, and that the mantle and inner core are perfectly elastic. We neglect the presence of oceans at the surface.

2.1 The Earth's external gravitational potential

The gravitational potential at a radius r outside an axisymmetric body of mean spherical radius a can be expressed as a sum of Legendre Polynomials (e.g. Jeffreys 1970):

$$\phi_{\rm g}(a,\theta) = -\frac{GM}{r}\left(1 - \sum_{n=2}\left(\frac{a}{r}\right)^n J_n P_n^0(\cos\theta)\right), \qquad (1)$$

where M is the mass of the Earth and the coefficients J_n are dimensionless numbers that represent the contribution of each zonal harmonic. In particular, J_2 is the coefficient of oblateness and represents the equatorial bulging of the Earth as a result of its own rotation. We note that $J_2 > 0$ represents an increase in oblateness. At the surface ($r = a$), the time variations of the J_n are related to the time-dependent zonal harmonic coefficients of the gravitational potential $\Phi_n^0(a, t)$ by

$$\Delta J_n(t) = \frac{a}{GM}\Delta\Phi_n^0(a,t). \qquad (2)$$

Here, we are interested solely in the changes in the gravitational potential of the whole Earth that result from the variations in geostrophic pressure along the CMB caused by torsional oscillations in the core and from changes in the mantle and inner core rotation rates.

2.2 Deformations in the mantle and inner core

Small displacements in the mantle and inner core caused by a load or an external forcing lead to changes in the stress field and gravity field. In turn, these changes create forces that induce additional

displacements and additional changes in the stress and gravity field. The resulting mechanical equilibrium in the deformed state is that for which the external force is balanced by the sum of the forces induced by the small displacements. In the present context, the forcing results from torsional oscillations in the fluid core or from changes in the rotation rate of the mantle and the inner core.

We follow the treatment of Dahlen (1972, 1974), except that we neglect the Coriolis force, assumed to be small in our problem, and we also eliminate the inertial terms because we are considering static perturbations. For a complete treatment of all the perturbation equations, we refer the reader to Dahlen & Trump (1998).

The mantle and inner core are assumed to be perfectly elastic and isotropic, although the elastic parameters and the density vary with depth. Their reference equilibrium configuration is defined in terms a zeroth-order balance relating the hydrostatic pressure $p_o(r)$, the density $\rho_o(r)$ and the gravitational potential $\phi_o(r)$. The undeformed mantle is assumed to be in hydrostatic equilibrium,

$$0 = -\frac{\partial}{\partial r} p_o(r) - \rho_o(r) g_o(r), \tag{3}$$

and the gravitational potential satisfies Poisson's equation,

$$\left(\frac{\partial^2}{\partial r^2} + \frac{2}{r}\frac{\partial}{\partial r}\right)\phi_o(r) = 4\pi G \rho_o(r). \tag{4}$$

In the above equilibrium state, the gravitational acceleration $-g_o(r)\,\mathbf{e_r}$ is defined in terms of the gravitational potential by $g_o(r) = \frac{\partial}{\partial r}\phi_o(r)$, and G is the gravitational constant. We note that this definition of the gravitational acceleration implies that the gravitational potential is *negative* everywhere.

The deformed state of the mantle is expressed in terms of small perturbations about the above equilibrium. The perturbations are created by small displacements $\mathbf{u}(\mathbf{r})$, which represent displacements of material particles from their position in the reference Earth (i.e. Lagrangian displacements). The displacements cause perturbations in the stress field and the gravitational potential. The static equilibrium of the deformed Earth is governed by an ensemble of conditions that comprise the momentum equation, which determines the mechanical equilibrium,

$$\mathbf{0} = \boldsymbol{\nabla}\cdot\mathbf{T} - \boldsymbol{\nabla}(\rho_o \mathbf{u}\cdot\boldsymbol{\nabla}\phi_o) - \rho_o\boldsymbol{\nabla}\phi_1 - \rho_1 g_o \mathbf{e_r} + \mathbf{f_e}, \tag{5}$$

an elastic constitutive relation,

$$\mathbf{T} = \lambda_o \mathbf{I}(\boldsymbol{\nabla}\cdot\mathbf{u}) + \mu_o[\boldsymbol{\nabla}\mathbf{u} + (\boldsymbol{\nabla}\mathbf{u})^{\mathrm{T}}], \tag{6}$$

an equation for continuity,

$$\rho_1 = -\rho_o \boldsymbol{\nabla}\cdot\mathbf{u} - \mathbf{u}\cdot\mathbf{e_r}\frac{\partial\rho_o}{\partial r}, \tag{7}$$

and Poisson's equation, which determines the changes in the gravity field,

$$\nabla^2\phi_1 = 4\pi G\rho_1. \tag{8}$$

The above set of four coupled equations is known as the set of linearized elastic-gravitational equations. The perturbations in the density $\rho_1 = \rho_1(\mathbf{u})$ and the gravitational potential $\phi_1 = \phi_1(\mathbf{u})$ are defined at fixed coordinate points $\mathbf{r}$, i.e. they are defined in a Eulerian reference frame. The incremental Lagrangian–Cauchy stress tensor $\mathbf{T} = \mathbf{T}(\mathbf{u})$ involves the second rank identity tensor $\mathbf{I}$, the Lamé parameter $\lambda_o = \lambda_o(r)$ and the modulus of rigidity $\mu_o = \mu_o(r)$. The latter two define the elastic state of the reference undeformed Earth. The externally applied body force $\mathbf{f_e} = \mathbf{f_e}(\mathbf{r})$ represents here the centrifugal force of the mantle rotation, which we write in terms of a centrifugal potential ϕ_c:

$$\mathbf{f_e} = -\rho_o\boldsymbol{\nabla}\phi_c. \tag{9}$$

The forcing from torsional oscillations will enter the perturbations in the mantle through the boundary conditions at the CMB.

Solutions of the above system are found by expanding $\mathbf{u}$, ϕ_1 and $\boldsymbol{\nabla}\cdot\mathbf{u}$ in terms of surface spherical harmonics as (e.g. Alterman *et al.* 1959)

$$\begin{aligned}
\mathbf{u} &= \sum_{n=0}^{\infty}\sum_{m=-n}^{n}\left(U_n^m(r)Y_n^m\mathbf{e_r} + V_n^m(r)\boldsymbol{\nabla}_1 Y_n^m\right),\\
\phi_1 &= \sum_{n=0}^{\infty}\sum_{m=-n}^{n}\Phi_n^m(r)Y_n^m,\\
\boldsymbol{\nabla}\cdot\mathbf{u} &= \sum_{n=0}^{\infty}\sum_{m=-n}^{n}\chi_n^m(r)Y_n^m,
\end{aligned} \tag{10}$$

where $\boldsymbol{\nabla}_1$ represents the gradient operator on the unit sphere:

$$\boldsymbol{\nabla}_1 = \mathbf{e}_\theta\frac{\partial}{\partial\theta} + \mathbf{e}_\varphi\frac{1}{\sin\theta}\frac{\partial}{\partial\varphi}. \tag{11}$$

The surface spherical harmonics Y_n^m are defined as

$$Y_n^m = Y_n^m(\theta,\varphi) = P_n^m(\cos\theta)\mathrm{e}^{im\varphi}, \tag{12}$$

where the functions $P_n^m(\cos\theta)$ are the associated Legendre polynomials. We use the following normalization over the unit sphere:

$$\int_\Omega Y_n^{m*}Y_s^t\,d\Omega = \frac{4\pi}{2n+1}\delta_{ns}\delta_{mt}. \tag{13}$$

This choice is convenient because for $m = 0$ it is equivalent to the Gauss–Schmidt normalization used in geomagnetism. This will facilitate the calculation of the perturbations directly in terms of the conventional definition of the flow coefficients at the CMB.

It is possible to write the complete set of elastic-gravitational equations in the mantle as a system of six coupled first-order ordinary differential equations (ODEs), for which a solution can be found with a numerical integration (Alterman *et al.* 1959). The set of equations is presented in Appendix A. In a compact notation, the system of ODEs can be written as

$$\frac{\partial}{\partial r}\mathbf{y} = \mathbf{A}\cdot\mathbf{y} + \mathbf{f}, \tag{14}$$

with the vector $\mathbf{y} = [y_1, y_2, y_3, y_4, y_5, y_6]^{\mathrm{T}}$, in which

$$\begin{aligned}
y_1 &= U_n^m\\
y_2 &= \lambda_o\chi_n^m + 2\mu_o\frac{\partial}{\partial r}U_n^m\\
y_3 &= V_n^m\\
y_4 &= \mu_o\left(\frac{\partial}{\partial r}V_n^m - \frac{V_n^m}{r} + \frac{U_n^m}{r}\right)\\
y_5 &= \Phi_n^m\\
y_6 &= \frac{\partial}{\partial r}\Phi_n^m + \frac{(n+1)}{r}\Phi_n^m + 4\pi G\rho_o U_n^m.
\end{aligned} \tag{15}$$

The interpretation of each quantity is as follows: y_1 and y_3 are respectively the radial and tangential displacements; y_2 and y_4 are respectively the radial and tangential stresses; y_5 is the gravitational potential; and y_6 is a gravitational acceleration.

The vector $\mathbf{f} = [f_1, f_2, f_3, f_4, f_5, f_6]^{\mathrm{T}}$ includes the externally applied body force. For our present case of a centrifugal force, the centrifugal potential ϕ_c is written in terms of a degree 2 zonal harmonic,

$$\phi_c = Z_2\frac{r^2}{a^2}Y_2^0, \tag{16}$$

where a is the radius of the Earth, and where $Z_2 = \Omega_o^2 a^2/3$ in the case of a centrifugal force of a body rotating at angular velocity Ω_o, or alternatively, $Z_2 = 2\Omega_o \delta\Omega a^2/3$ in the case of a centrifugal force associated with an angular velocity change of $\delta\Omega$. Using the above decomposition of ϕ_c in (9) yields a forcing vector $\mathbf{f}$ for which the only non-zero contributions are

$$f_2 = \rho_o \frac{\partial}{\partial r}\left(Z_2 \frac{r^2}{a^2}\right) = 2\rho_o Z_2 \frac{r}{a^2},$$
$$f_4 = \rho_o Z_2 \frac{r}{a^2}, \tag{17}$$

and restricted to harmonic degree 2.

The perturbations in the inner core are treated in an equivalent manner to those in the mantle. The set of elastic-gravitational equations in the inner core is

$$\frac{\partial}{\partial r}\mathbf{y}^s = \mathbf{A}\cdot\mathbf{y}^s + \mathbf{f}^s, \tag{18}$$

where $\mathbf{y}^s$ is the solution vector in the inner core and $\mathbf{f}^s$ is defined identically to $\mathbf{f}$ except that it represents the centrifugal force in the inner core. As for the mantle, the forcing from torsional oscillations enters the inner core equations through the boundary conditions at the ICB.

2.3 Deformations in the fluid core caused by torsional oscillations

The undeformed static reference state in the core is isotropic and spherically symmetric. As for the mantle and the inner core, the equilibrium between the hydrostatic pressure, the density and the gravitational potential is determined in terms of the hydrostatic balance (3) and Poisson's equation (4).

The perturbations in the gravity field in the core that result from small displacements differ than those in the solid Earth because tangential stresses vanish everywhere. The appropriate way of calculating the perturbations in the static limit has been the subject of intense debate in the literature and is known as 'Longman's paradox', or 'static core paradox' (Longman 1963; Jeffreys & Vicente 1966; Smylie & Mansinha 1971; Pekeris & Accad 1972; Israel *et al.* 1973; Dahlen 1974; Chinnery 1975; Crossley & Gubbins 1975; Dahlen & Fels 1978). The controversy arises as a result of the absence of rigidity in the core. In the static limit with $\mu_o = 0$, the above elastic-gravitational equations have no solutions unless the liquid core is assumed to be neutrally stratified or deformations are assumed to be divergence-free, neither case being completely physically realistic. One way to understand the difficulty is as follows. In the absence of shear stresses, displacements of fluid particles in the core must coincide with the deformations of surfaces of constant gravitational potential. In the mantle, however, displacements result from the combined effects of changes in gravitational potential and elastic strain. Yet, the gravitational potential must be continuous across the CMB. Hence, if the equilibrium shape of the CMB satisfies the displacements on the mantle side, this surface does not match a surface of constant gravitational potential. In other words, fluid particles next to the CMB are no longer on their original gravitational potential surface, and unless the core is neutrally stratified, they experience a buoyancy force which prevents a static equilibrium. Recent discussions on the static-core paradox can be found in the work of Fang (1998) and Denis *et al.* (1998). However, in the case of a spherically symmetric Earth model, as it applies in this study, if one assumes that displacements are divergence-free, the neutrally stratified condition necessarily follows and a static solution is possible, although the displacements of individual fluid particles cannot be uniquely determined (e.g. Denis *et al.* 1998). Dahlen (1974), Chinnery (1975), and Crossley & Gubbins (1975) showed that an equivalent resolution of the difficulty is obtained by requiring that the hydrostatic equilibrium in the fluid core is maintained at all times. In this case, displacements in the core can be determined and still be represented using a Lagrangian description, but only provided that they be interpreted as the displacement of equipotential surfaces, not the displacement of actual fluid particles. Here, we follow their approach, which is also used in postglacial rebound studies (e.g. Wu & Peltier 1982), and is valid for problems for which the typical timescales of the variations are much longer than the gravest of the normal modes of oscillation of the Earth (Dahlen & Fels 1978).

If hydrostatic equilibrium is maintained even in the deformed state, the surfaces of constant density, constant fluid pressure and constant gravitational potential always coincide. The fluid displacements parallel to the equipotential surfaces are undetermined. The static equilibrium in the core under small (Lagrangian) displacements $\mathbf{u}(\mathbf{r})$ of the equipotential surfaces is governed by the linearized first-order perturbations in the hydrostatic balance,

$$\mathbf{0} = -\nabla p_1 - \rho_o \nabla\phi_1 - \rho_1 g_o \mathbf{e_r} + \mathbf{f_e}, \tag{19}$$

the linearized first-order Poisson's equation,

$$\nabla^2\phi_1 = 4\pi G\rho_1, \tag{20}$$

and an equation for continuity,

$$\rho_1 = -u_r \frac{\partial\rho_o}{\partial r}, \tag{21}$$

in which we have used the divergence-free condition, $\nabla\cdot\mathbf{u} = 0$. As for the solid Earth, $\rho_1 = \rho_1(\mathbf{u})$, $\phi_1 = \phi_1(\mathbf{u})$, and $p_1 = p_1(\mathbf{u})$ are all Eulerian variables. Here, $\mathbf{f_e} = \mathbf{f_e}(\mathbf{r})$ is the radial force from torsional oscillations acting on the equipotential surfaces. This force is equivalent to the Coriolis force associated with the torsional oscillation velocity $\mathbf{v} = v_\varphi \mathbf{e}_\varphi$, and is given by $\mathbf{f_e} = -2\rho_o \boldsymbol{\Omega}\times\mathbf{v}$, where $\boldsymbol{\Omega} = \Omega_o \mathbf{e}_z$ is the angular velocity of the Earth's rotation.

Torsional oscillations are azimuthal flows for which the quantity $\rho_o v_\varphi \mathbf{e}_\varphi$ is independent of z, the coordinate parallel to the rotation axis. The Coriolis force associated with this type of flow is conservative, because

$$\nabla\times(\boldsymbol{\Omega}\times\rho_o\mathbf{v}) = \boldsymbol{\Omega}(\nabla\cdot\rho_o\mathbf{v}) - \boldsymbol{\Omega}\cdot\nabla\rho_o\mathbf{v} = -\Omega_o\frac{\partial}{\partial z}\rho_o\mathbf{v} = \mathbf{0}. \tag{22}$$

We can therefore express it as a gradient of a potential, $2\,\boldsymbol{\Omega}\times\rho_o\,\mathbf{v} = -\,\nabla p_g$, where we call p_g the geostrophic pressure. The perturbation in the hydrostatic balance (19) can then be written as

$$\mathbf{0} = -\nabla(p_1 - p_g) - \rho_o\nabla\phi_1 - \rho_1 g_o \mathbf{e_r}. \tag{23}$$

By decomposing (23) into its radial and transverse components and using (21), it follows that

$$p_1 = -\rho_o\phi_1 + p_g, \tag{24}$$

$$u_r = -\frac{\phi_1}{g_o}. \tag{25}$$

Eqs (21), (24) and (25) represent the coherent displacements of surfaces of constant density, gravitational potential, and the combination of the pressure and geostrophic pressure.

By inserting (21) and (25) in (20), we obtain a second-order linear differential equation for ϕ_1:

$$\nabla^2\phi_1 = \frac{4\pi G}{g_o}\frac{\partial\rho_o}{\partial r}\phi_1. \tag{26}$$

This version of Poisson's equation implies that the perturbations in the gravitational potential within the core are independent of the local geostrophic forcing. The geostrophic forcing creates the disturbances in ϕ_1 by displacing the solid–fluid boundaries, and enters the system through the boundary conditions that will be specified in Section 2.5. The changes in ϕ_1 within the core are entirely a consequence of the disturbances at the boundaries. Once a solution for ϕ_1 is obtained, the displacement of equipotential surfaces u_r and the perturbations in pressure p_1 may be subsequently determined from the known p_g.

The solutions of this equation can be found by expanding ϕ_1 in spherical harmonics:

$$\phi_1 = \sum_{n=0}^{\infty} \sum_{m=-n}^{n} \Phi_n^m(r) Y_n^m. \tag{27}$$

Upon substitution of (27), (26) separates into a set of equations in $\Phi_n^m(r)$ for each n and m, namely

$$\frac{\partial^2 \Phi_n^m}{\partial r^2} + \frac{2}{r}\frac{\partial \Phi_n^m}{\partial r} - \left(\frac{n(n+1)}{r^2} + \frac{4\pi G}{g_o}\frac{\partial \rho_o}{\partial r} \right) \Phi_n^m = 0. \tag{28}$$

It is convenient to rewrite (28) in a form similar to the set of equations that determine the perturbations in the solid Earth. This will later facilitate the implementation of the boundary conditions and the solution of the entire problem. We therefore use the same change of variable,

$$\begin{aligned} y_5^c &= \Phi_n^m \\ y_6^c &= \frac{\partial y_5^c}{\partial r} - \frac{4\pi G \rho_o}{g_o} y_5^c + \frac{n+1}{r} y_5^c, \end{aligned} \tag{29}$$

where the superscript c is used to identify fluid core variables, and where we have used (25) for the radial displacement y_1^c.

Eq. (28) can be written as a coupled ODE system in terms of y_5^c and y_6^c. In matrix form, with $\mathbf{y}^c = [y_5^c, y_6^c]^T$, we get

$$\frac{\partial}{\partial r}\mathbf{y}^c = \mathbf{B} \cdot \mathbf{y}^c, \tag{30}$$

where

$$\mathbf{B} = \begin{pmatrix} \frac{4\pi G \rho_o}{g_o} - \frac{n+1}{r} & 1 \\ \frac{8\pi G \rho_o}{g_o}\frac{(n-1)}{r} & \frac{(n-1)}{r} - \frac{4\pi G \rho_o}{g_o} \end{pmatrix}. \tag{31}$$

The above development is equivalent to that presented by Wu & Peltier (1982). The changes in $\mathbf{y^c}$ that result from both the torsional oscillations and the variations in the rotation rate of the mantle and inner core will enter the above equations through the boundary conditions at the CMB and ICB.

2.4 Geostrophic pressure

The geostrophic pressure that produces the distortion of the CMB is completely determined by torsional oscillations. We now wish to express the spherical harmonic coefficients of the geostrophic pressure in terms of this flow. As we defined above,

$$2\boldsymbol{\Omega} \times (\rho_o \mathbf{v}) = -\boldsymbol{\nabla} p_g. \tag{32}$$

Torsional oscillations are purely azimuthal flows, $\mathbf{v} = v_\varphi \mathbf{e}_\varphi$, and therefore

$$2\Omega_o \rho_o v_\varphi \mathbf{e_s} = \boldsymbol{\nabla} p_g, \tag{33}$$

where $\mathbf{e_s}$ is the direction perpendicular to the rotation axis. The geostrophic pressure is a function only of s, the distance from the rotation axis. In other words, p_g is constant along lines parallel to the rotation axis. The value of p_g at any point in the core may then be determined by an axial projection of its value at the CMB. This allows a determination of p_g in terms of a torsional oscillation flow represented at the CMB. Such a relationship is easily obtained by taking $\mathbf{e_r} \times$ (33), which gives

$$2\Omega_o b \rho_o \cos\theta v_\varphi \mathbf{e}_\varphi = \mathbf{e_r} \times \boldsymbol{\nabla}_1 p_g, \tag{34}$$

where b is the radius of the CMB, and $\boldsymbol{\nabla}_1$ is defined on a unit sphere.

We first require a representation of the core surface flow v_φ in a spherical harmonic decomposition. The general representation of the tangential velocity at the CMB obtained from the geomagnetic field secular variation is usually written in terms of a toroidal and poloidal decomposition (e.g. Bloxham & Jackson 1991),

$$\mathbf{v_h} = \mathbf{v}_T + \mathbf{v}_P = \boldsymbol{\nabla}_1 \times (\mathcal{T}\mathbf{e_r}) + \boldsymbol{\nabla}_1 \mathcal{S}, \tag{35}$$

where $\mathcal{S}$ and $\mathcal{T}$ are respectively the poloidal and toroidal scalars which are expanded in spherical harmonics. For torsional oscillations, the only non-zero contributions are from the zonal toroidal components that are symmetric about the equator. Hence the spherical harmonic decomposition is limited to the coefficients t_n^0 for *n odd*,

$$\begin{aligned} &\mathbf{v_h} = v_\varphi \mathbf{e}_\varphi = \boldsymbol{\nabla}_1 \times (\mathcal{T}\mathbf{e_r}) = -\mathbf{e_r} \times \boldsymbol{\nabla}_1 \mathcal{T}, \\ &\mathcal{T} = \sum_{nodd} t_n^0 Y_n^0. \end{aligned} \tag{36}$$

We note that, in geomagnetism, the expansion of $\mathcal{T}$ and $\mathcal{S}$ is usually done in terms of real spherical harmonics instead of our choice defined in (12). However, the two expansions are identical for the zonal harmonics. The coefficients t_n^0 in (36) are therefore equivalent to those given by CMB flow inversion studies. We also note that the coefficients t_n^0 are defined in this study with respect to a reference frame rotating at angular velocity Ω_o.

With (34), we can relate the spherical harmonic coefficients of the geostrophic pressure at the CMB, $\Psi_n^m(b)$, defined as

$$p_g(b) = \sum_{n=0}^{\infty} \sum_{m=-n}^{n} \Psi_n^m(r) Y_n^m, \tag{37}$$

to the coefficients of torsional oscillations defined above in (36) (Gire & Le Mouël 1990). The details of the derivation of this relationship are presented in Appendix B. The only non-zero coefficients of the geostrophic pressure are those with both $m = 0$ and *n even*. This is consistent with our expectation that torsional oscillations produce perturbations that are axisymmetric and symmetric about the equator. In Appendix B, we demonstrate the more general result that torsional oscillations are in fact the only component of the flow that produce changes in the even zonal harmonics of the geostrophic pressure at the CMB. Here, we simply present the result: for an *even* degree n, the coefficients $\Psi_n^0(b)$ are given by

$$\Psi_n^0(b) = -\Omega_o b \rho_o \left(\frac{2(n-1)}{(2n-1)} t_{n-1}^0 + \frac{2(n+2)}{(2n+3)} t_{n+1}^0 \right). \tag{38}$$

Hence, the zonal geostrophic pressure coefficient at a given n depends only on two coefficients of the flow, t_{n-1}^0 and t_{n+1}^0 (Gire & Le Mouël 1990).

To complete the problem, we also need to compute the coefficients $\Psi_n^0(c)$ that represent the geostrophic pressure at the ICB ($r = c$). Because the only non-zero coefficients are those with $m = 0$, we can expand the geostrophic pressure in terms of Legendre polynomials as

$$p_g(c, \theta) = \sum_{neven} \Psi_n^0(c) P_n^0(\cos\theta), \tag{39}$$

and relate the coefficients $\Psi_n^0(c)$ to the coefficients $\Psi_n^0(b)$ defined at the CMB in (38). Because the geostrophic pressure is constant on *cylindrical* surfaces aligned with the rotation axis, this is done by taking the axial projection of the Legendre polynomial expansion at the CMB onto the interior radius c,

$$p_{\rm g}(c,\theta) = \sum_{n' even} \Psi^0_{n'}(b) P^0_{n'}\left(\cos\left(\arcsin\left(\frac{c}{b}\sin\theta\right)\right)\right), \tag{40}$$

and expanding this latter expression in terms of Legendre polynomials defined on the interior radius c. Equating (39) and (40) gives the contribution of the CMB coefficient at degree n' to the ICB coefficient at degree n. We note that as a result of the axial projection, we expect that the coefficients $\Psi_n^0(c)$ also contain contributions from coefficients of *higher* harmonic degrees n' of the forcing defined at the CMB.

The determination of the $\Psi_n^0(c)$s according to the above scheme is relatively straightforward. However, compared with the CMB deformations, the effects on the gravity field at the surface caused by the distortion of the ICB are much smaller. This is because the density jump is smaller at the ICB, and more important, because the perturbations created at the ICB are more attenuated when they reach the surface than those created at the CMB. We have verified that the inclusion of the ICB deformation has a negligible effect on the results of this study. Therefore, for the sake of simplicity, we have decided to neglect the effects of the geostrophic pressure at the ICB, and from now on we assume that $\Psi_n^0(c) = 0$.

2.5 Boundary conditions

The solution of the coupled ODEs for the perturbations in the core in (30) depends upon two constants of integration. Likewise, the solution for the perturbations in the mantle in (14) and in the inner core in (18) each require six constants of integration. These 14 degrees of freedom are specified in terms of boundary conditions at the origin, the ICB, the CMB, and the Earth's surface.

The conditions that the variables of our system have to obey at these interfaces are as follows. At each discontinuity in density or elastic parameters, including those at the Earth's surface, the gravitational potential ϕ_1 and the gravitational flux $\mathbf{e}_{\rm r}\cdot(\boldsymbol{\nabla}\phi_1 + 4\pi G\rho_{\rm o}\mathbf{u})$ must be continuous. At internal boundaries between two solid regions, all displacements and traction forces must be continuous. At a boundary between a solid and inviscid fluid, tangential displacements may be allowed. The traction force must still be continuous at a fluid–solid boundary, but since an inviscid fluid cannot support shear, the tangential traction vanishes at the boundary. At the Earth's surface, in the absence of surface load, the traction forces must vanish.

The above requirements impose that, at radial surfaces in the mantle and the inner core where there exists a discontinuity in $\rho_{\rm o}$, $\lambda_{\rm o}$ or $\mu_{\rm o}$, all six y_i's are continuous. At the CMB, the appropriate way of incorporating the above conditions has been discussed by a number of authors and is related to the static-core paradox (see earlier references). As mentioned above, the difficulty stems from the fact that deformations in the core coincide with displacements of equipotential surfaces, whilst this is generally not the case in the mantle. Consequently, fluid particles next to the CMB cannot be on their original equipotential surface and experience a buoyancy force. Yet, on long timescales, after dissipation of the oscillations that ensue from this restoring buoyancy force, the density of individual fluid particles is altered by Newtonian cooling and they can rest on a different equipotential surface (Dahlen & Fels 1978). In other words, on long timescales the core behaves as if it were neutrally stratified. Hence, in our formalism where we are not interested in the static displacements of individual fluid particles but only in the equilibrium deformation of the equipotential surfaces, the latter do not have to match the shape of the CMB. Allowance for this is incorporated by introducing an apparent jump in the radial displacement at the CMB in terms of an arbitrary constant. The complete set of boundary conditions at the CMB is

$$\begin{aligned}
y_1(b) &= -\frac{y_5^{\rm c}(b)}{g_{\rm o}(b)} + C_5,\\
y_2(b) &= C_5 g_{\rm o}(b)\rho_{\rm o}(b^-) - \Psi_n^0(b),\\
y_3(b) &= C_4,\\
y_4(b) &= 0,\\
y_5(b) &= y_5^{\rm c}(b),\\
y_6(b) &= y_6^{\rm c}(b) + 4\pi G\rho_{\rm o}(b^-)C_5,
\end{aligned} \tag{41}$$

where (b^-) indicates a quantity evaluated in the fluid side of the boundary. The constant C_5 represents the apparent jump in radial displacement, and C_4 is the arbitrary tangential displacement at the base of the mantle. The boundary condition on the radial stress (y_2) introduces the forcing from the geostrophic pressure in the system. The radial stress on the fluid side includes the geostrophic pressure (it is given by 24), which leads to the above condition.

By analogy, a similar set of boundary conditions applies at the ICB. However, because the method of solution involves an integration of the perturbation equations from $r \to 0$ towards the external radius, the boundary conditions at the ICB are manipulated into a more convenient form. In the fluid core, we are only concerned about $y_5^{\rm c}$ and $y_6^{\rm c}$, and the propagation of these two variables across the ICB is given by

$$\begin{aligned}
y_5^{\rm c}(c) &= y_5^{\rm s}(c),\\
y_6^{\rm c}(c) &= y_6^{\rm s}(c) - \frac{4\pi G}{g_{\rm o}(c)}\left(y_2^{\rm s}(c) + \Psi_n^0(c)\right),
\end{aligned} \tag{42}$$

where we have used the condition on y_2 across the ICB. Two additional conditions must be obeyed by the solution in the inner core at the ICB:

$$y_4^{\rm s}(c) = 0, \tag{43}$$

$$g_{\rm o}(c)\rho_{\rm o}(c^+)y_1^{\rm s}(c) - y_2^{\rm s}(c) + \rho_{\rm o}(c^+)y_5^{\rm s}(c) - \Psi_n^0(c) = 0, \tag{44}$$

where (c^+) indicate a quantity evaluated on the fluid side of the ICB, and where the second of these condition is obtained from combining the conditions on y_1 and y_2. According to our approximation in the previous section, we set $\Psi_n^0(c) = 0$ in the last two sets of equations.

The conditions that ensure that the solution in the inner core remains finite as $r \to 0$ can be determined by an analytical solution near the origin. Following Crossley (1975), if we assume that near the origin $\partial\rho/\partial r \to 0$, then $g_{\rm o} \to 4\pi G\rho_{\rm o} r/3$, and an analytical solution can be obtained by a power-series expansion of the variables. The solution of the six variables at a small radius ϵ depends on three independent coefficients, and the solution can be written as

$$\mathbf{y}^{\rm s}(\epsilon) = C_1\mathbf{y}^{\boldsymbol{\epsilon 1}} + C_2\mathbf{y}^{\boldsymbol{\epsilon 2}} + C_3\mathbf{y}^{\boldsymbol{\epsilon 3}}. \tag{45}$$

The coefficients C_1, C_2 and C_3 are three additional constants of integration and the vectors $\mathbf{y}^{\epsilon 1}$, $\mathbf{y}^{\epsilon 2}$ and $\mathbf{y}^{\boldsymbol{\epsilon 3}}$ are given in Appendix C.

At the top of the mantle, in the absence of any external load, the radial stresses, the tangential stresses and the gravitational flux all vanish, which specifies three additional conditions:

$$y_2(a) = y_4(a) = y_6(a) = 0. \tag{46}$$

We therefore have a total of 19 boundary conditions, which are specified in terms of five constants. The values of these constants are those for which all 19 boundary conditions can be simultaneously satisfied. The determination of the constants removes five degrees of freedom in the system and allows a unique solution for the whole problem. The solution can be found by integrating (18) from a small r, using (45) as a starting solution. The boundary conditions (42) at the ICB are applied and the solution is propagated in the core with (30). The set of boundary conditions at the CMB are applied and the solution is propagated to the surface with (14). The integration is iterated by varying the five constants until the conditions (43) and (44) at the ICB and the three boundary conditions at the surface (46) are all satisfied.

2.6 Love numbers

The contribution of the torsional oscillations to the perturbations from the reference state is determined by setting $Z_2 = 0$ in (16). From a known torsional oscillation flow model, the coefficients $\Psi_n^0(b)$ for the forcing at degree n on the CMB are determined by (38). It is useful to represent the perturbation in the gravitational potential at the surface $\Phi_n^0(a)$ in terms of $\Psi_n^0(b)$ by casting the whole problem under the formalism of Love numbers (Love 1909). Let us define

$$\Phi_n^0(a) = -k_n \frac{\Psi_n^0(b)}{\bar{\rho}}, \tag{47}$$

where the Love number k_n represents the gravitational potential perturbation at harmonic degree n at the surface of the Earth that results from a geostrophic pressure of the same degree at the CMB. For a normalization of our system of equations with typical scales for r, g_o and ρ_o given respectively by a, $\bar{g}$ and $\bar{\rho}$, where $\bar{g}$ is the acceleration at the surface and $\bar{\rho}$ is the mean density of the Earth, the Love numbers k_n are then simply the solution for variable y_5 at $r = a$ for $\Psi_n^0(b) = 1$ and neatly summarize the effects of elastic deformation of the whole planet.

The perturbation in gravitational potential that results from the change in rotation rate of the mantle can similarly be expressed in terms of a Love number representation. For the centrifugal potential given by (16), we define

$$\Phi_2^0(a) = k_m Z_2^{(m)}, \tag{48}$$

so that k_m represents the amplitude of the gravity field perturbation of degree 2 at the surface that results from a centrifugal potential in the mantle that has unit amplitude at the surface, i.e. $Z_2^{(m)} = 1$. Likewise, we define

$$\Phi_2^0(a) = k_{ic} Z_2^{(ic)}. \tag{49}$$

Hence, k_{ic} represents the amplitude of the gravity field perturbation of degree 2 at the surface that results from a centrifugal potential in the inner core with $Z_2^{(ic)} = 1$. We note that $Z_2^{(ic)}$ is set to zero to calculate k_m (and vice versa), and that in both cases the torsional oscillations forcing is set to zero.

We define similar Love numbers to characterize the radial displacements at the surface $D_n^0(a)$:

$$D_n^0(a) = h_n \frac{\Psi_n^0(b)}{\bar{\rho}\bar{g}},$$

$$D_2^0(a) = -h_m \frac{Z_2^{(m)}}{\bar{g}},$$

$$D_2^0(a) = -h_{ic} \frac{Z_2^{(ic)}}{\bar{g}}. \tag{50}$$

3 RESULTS

The solutions depend on the reference Earth model upon which the perturbations are imposed. We use here the Earth model PREM (Dziewonski & Anderson 1981) which specifies a radially symmetric Earth with a reference density $\rho_o(r)$ (from which a gravitational acceleration $g_o(r)$ and gravitational potential $\phi_o(r)$ are determined), and elastic parameters $\lambda_o(r)$ and $\mu_o(r)$ for every radial surface. The outermost region in PREM represents an overriding ocean. For now, we simply neglect the additional dynamical effects of oceans and extend the parameters of the previous region (crust) to this outermost radius. In Table 1 we list the values of all other relevant parameters used in our calculations.

3.1 Solutions of the perturbation problem

The degree 2 zonal harmonic perturbation of y_1 and y_5 as a function of radius that result from a centrifugal potential with $Z_2^{(m)} = 1$ in the mantle and zero forcing in the fluid core and inner core are presented in Fig. 5 (thick line). For a comparison, we have also plotted the solutions obtained for a centrifugal force acting everywhere in the Earth (thin line). We note that each variable has been normalized so that the solution at the surface equals the Love numbers k_m and h_m, and we find $k_m = 0.2345$ and $h_m = 0.4769$. To get the dimensional value of y_5, one needs to multiply the values in Fig. 5 by the dimensional amplitude of the forcing potential. The dimensional value of y_1 is obtained by multiplying the result by the forcing potential divided by $\bar{g}$.

The solution of y_1 and y_5 as a function of radius that results from a centrifugal potential with $Z_2^{(ic)} = 1$ in the inner core and zero forcing in the fluid core and mantle is presented in Fig. 6. The solutions at the surface determine k_{ic} and h_{ic}, and we find $k_{ic} = 1.47 \times 10^{-6}$ and $h_{ic} = 1.29 \times 10^{-6}$. Compared with the previous solution, the amplitudes of y_1 and y_5 are much smaller. The change in the elliptical gravity field and radial displacement at the surface is 5 orders of magnitude larger for a change in mantle rotation rate than for an equivalent change in inner core rotation rate. This difference is in part because for an equivalent change in rotation rate, the forcing at the surface is roughly 25 times larger than at the ICB. The remaining part of the discrepancy is mostly a consequence of the smaller density jump at the ICB and the attenuation of the perturbation as it propagates to the surface.

We now solve for the perturbations that result from the forcing of torsional oscillations in the core. We set $Z_2^{(m)} = Z_2^{(ic)} = 0$, and compute the perturbations at degree n in the whole Earth that result from a torsional oscillation flow that produces a unit amplitude geostrophic pressure of the same degree at the CMB, i.e. $\Psi_n^0(b) = 1$. In Fig. 7, we present the solution of the perturbation in radial

Table 1. Parameters used in the calculations.

Parameter	Value
Gravitational constant	$G = 6.67 \times 10^{-11}$ m^3 kg^{-1} s^{-2}
Mass of the Earth	$M = 5.97 \times 10^{24}$ kg
Earth's rotation rate	$\Omega_o = 7.29 \times 10^{-5}$ s^{-1}
Moment of inertia of the mantle	$I_m = 7.12 \times 10^{37}$ kg m^2
Moment of inertia of the core	$I_c = 0.92 \times 10^{37}$ kg m^2
Radius of Earth	$a = 6.371 \times 10^6$ m
Radius of the core	$b = 3.480 \times 10^6$ m
Radius of the inner core	$c = 1.2215 \times 10^6$ m
Acceleration at the surface	$\bar{g} = GM/a^2 = 9.82$ m s^{-2}
Mean density	$\bar{\rho} = 5515$ kg m^{-3}

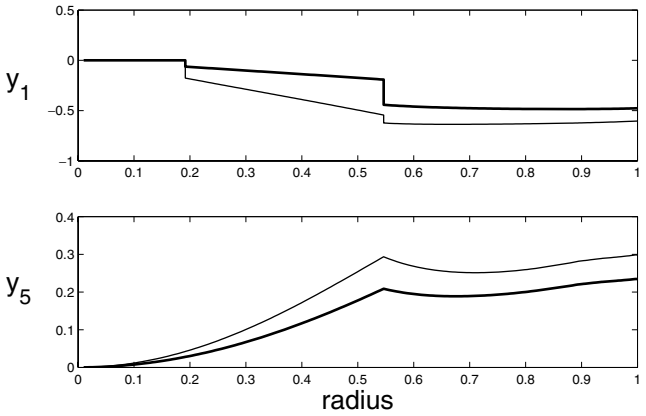

Figure 5. Solution of the zonal spherical harmonic coefficient of degree 2 of the radial displacement y_1, and of the perturbation in gravitational potential y_5 as a function of radius for a centrifugal force acting on the mantle only (thick line), and for a centrifugal force acting on the whole Earth (thin line). Solutions are dimensionless. We recall that y_1 represents the displacements of material surfaces in the inner core ($0 \leq r \leq 0.1917$) and the mantle ($0.5462 \leq r \leq 1$) but is defined as the displacements of equipotential surfaces in the fluid core ($0.1917 < r < 0.5462$).

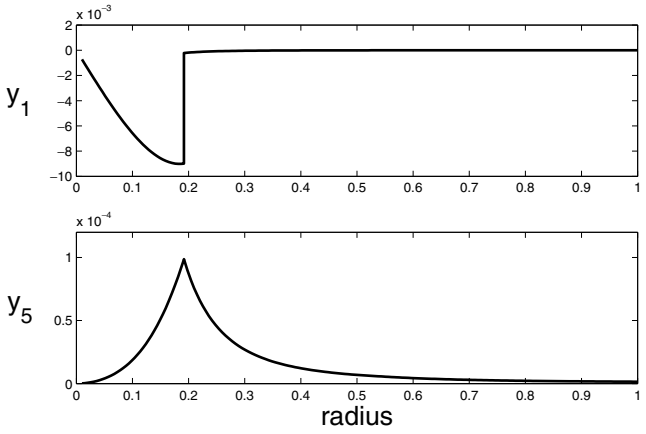

Figure 6. As Fig. 5, but for a centrifugal force that acts only on the inner core.

displacement and gravitational potential for $n = 2$. The solutions at the surface give, respectively, the Love numbers k_2 and h_2. We find $k_2 = 0.1116$ and $h_2 = 0.2302$.

The dimensional value of y_5, when the forcing is from the geostrophic pressure, is obtained by multiplying the results by the dimensional applied geostrophic pressure divided by $\bar{\rho}$. Similarly, the dimensional value of y_1 is obtained by multiplying the results by the dimensional applied geostrophic pressure divided by $\bar{\rho}\bar{g}$. An estimate of the amplitude of the vertical displacement and change in gravity at the surface of the Earth produced by our model is easily obtained from Fig. 7. The geostrophic pressure scales as $\Psi \sim \rho_o \Omega_o b v_{to}$, and a typical amplitude of the change in torsional oscillation velocity is about a kilometre per year ($v_{to} \sim 3 \times 10^{-5}$ m s^{-1}). Hence, the normalized radial displacements in the core shown in Fig. 7, $y_1 \sim 0.1$, correspond to dimensional displacements of $(1/10)\rho_o \Omega_o b v_{to}/\bar{\rho}\bar{g}$, which gives ~ 0.15 mm. The vertical displacements of the CMB and the Earth's external surface are $\sim$0.5 mm and $\sim$0.35 mm respectively. The gravitational potential change at the Earth's surface corresponds to an equivalent change in geoid height of $k_2 \rho_o \Omega_o b v_{to}/\bar{\rho}\bar{g}$, which gives $\sim$0.15 mm.

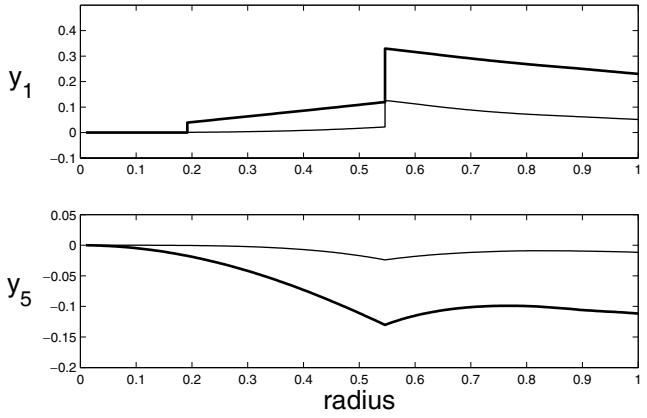

Figure 7. Solution of y_1 and y_5 (dimensionless) as a function of radius for a geostrophic pressure at the CMB of $\Psi_2^0(b) = 1$ (thick line) and $\Psi_4^0(b) = 1$ (thin line).

Table 2. Love numbers.

k_m	$= 2.345 \times 10^{-1}$	h_m	$= 4.769 \times 10^{-1}$
k_{ic}	$= 1.47 \times 10^{-6}$	h_{ic}	$= 1.29 \times 10^{-6}$
k_2	$= 1.116 \times 10^{-1}$	h_2	$= 2.302 \times 10^{-1}$
k_4	$= 1.156 \times 10^{-2}$	h_4	$= 5.135 \times 10^{-2}$
k_6	$= 1.957 \times 10^{-3}$	h_6	$= 1.366 \times 10^{-2}$
k_8	$= 4.171 \times 10^{-4}$	h_8	$= 4.013 \times 10^{-3}$

The solution obtained at degree $n = 4$ is also shown in Fig. 7. The results are similar to those obtained with $n = 2$ but with smaller amplitudes. The values of the Love numbers for $n = 4$ are $k_4 = 0.01156$ and $h_4 = 0.05135$. The Love numbers for a few of the larger harmonics are presented in Table 2.

3.2 Time variations in the zonal harmonics of the gravity field

With the Love numbers calculated above, the perturbations in even degree n of the gravitational potential at the surface can be readily obtained for a given model of torsional oscillations. Since the flow is time-dependent, the variations in time at the surface are then obtained from the instantaneous torsional oscillation flow at each time step. Using (2), (47), (48) and (49), the variations in the coefficients J_n, for $n > 2$, are then given by

$$\Delta J_n(t) = -k_n \frac{a}{GM} \frac{\Psi_n^0(b,t)}{\bar{\rho}}, \tag{51}$$

and the variations in J_2 are given by

$$\Delta J_2(t) = \frac{a}{GM}\left(-k_2 \frac{\Psi_n^0(b,t)}{\bar{\rho}} + k_m Z_2^{(m)}(t) + k_{ic} Z_2^{(ic)}(t)\right). \tag{52}$$

Let us first consider the role of a change in inner core rotation rate in the variations in J_2. We found k_{ic} to be 5 orders of magnitude smaller than k_m. In other words, the changes in rotation rate of the inner core have to be 5 orders of magnitude larger than the changes in rotation rate of the mantle for the former to play a role as important as the latter in the variations in J_2. We can estimate directly the variations in J_2 caused by changes in inner core rotation rate $\delta\Omega_{ic}$ by using $Z_2^{(ic)} = 2\Omega_o \delta\Omega_{ic} a^2/3$ in (52):

$$\Delta J_2 = \frac{2}{3}\frac{a^3 \Omega_o}{GM} k_{ic} \delta\Omega_{ic}. \tag{53}$$

Using the values in Table 1, and $k_{ic} = 1.47 \times 10^{-6}$, this implies that $\Delta J_2 \approx \delta\Omega_{ic} \times 10^{-5}$ s. Hence, in order to produce changes in J_2 of the scale of the '1998 anomaly' (10^{-10}), we need a change in rotation rate of the inner core of the order of 10^{-5} s^{-1}, or $\approx 1/7$ of the actual rotation rate of the Earth. So, for instance, considering a 10^{-10} per year change in J_2 for 3 yr, the required rotation rate change of the inner core would have rotated it by 180° with respect to the mantle!

Such a high rotation rate of the inner core is unrealistic because it is 2 orders of magnitude larger than the largest estimates inferred from seismology (Song & Richards 1996; Su *et al.* 1996), and 3 orders of magnitude larger than more conservative estimates (Laske & Masters 1999; Souriau & Poupinet 2000). Physically, it is also very unlikely because the inner core is tightly coupled electromagnetically to the fluid core (Gubbins 1981) and gravitationally to the mantle (Buffett 1996). Zatman (2003) estimated the change in rotation rate of the inner core by assuming perfect coupling at the ICB with the rigid cylindrical flows inside the tangent cylinder. He obtained changes of order 0.3° yr^{-1}, or $\delta\Omega_{ic} \approx 1.6 \times 10^{-10}$ s^{-1}. While it is questionable whether the assumption of perfect coupling at the ICB is valid and whether the flow inside the tangent cylinder can be well recovered in the data, this value is nevertheless a good approximation of the amplitude of $\delta\Omega_{ic}$. Indeed, this is also the predicted amplitude of $\delta\Omega_{ic}$ if a large part of the length-of-day variations result from free oscillations between the mantle, inner core and torsional oscillations (Mound & Buffett 2003). Such a change in rotation rate of the inner core would produce changes in J_2 of the order of 10^{-15}, clearly too small to be observable. Since the above considerations suggest that the inner core has a negligible role in the changes in J_2, and since we do not have reliable observations of the variations of inner core rotation rate at decade periods, for convenience we neglect its contribution in (52).

The remaining terms in (52) can be conveniently reorganized. As we pointed out in the Introduction, our confidence in torsional oscillations stems from the good agreement between the observed changes in the length of day (ΔT) and those predicted from the changes in core angular momentum that they carry. It turns out that the geostrophic pressure can be expressed directly in terms of ΔT, as we demonstrate below. Similarly, the centrifugal potential in the mantle is also directly proportional to ΔT. This allows us to rewrite (52) and express the changes in J_2 as a function of changes in the length of day alone.

Let us first consider how torsional oscillations are related to ΔT. In what follows, we make the assumption that changes in the axial angular momentum in the core $L_c(t)$ and the mantle $L_m(t)$ are due solely to variations in their respective rotation rates. In other words, the axial moments of inertia of the core I_c and the mantle I_m remain constant. (We note that the variations in axial angular momentum produced by the secondary effect of changes in the moments of inertia due to changes in the rotation rate are of the order of a factor 300 smaller.) Measured in a reference frame fixed to the mantle, the change in angular momentum in the core is carried by only two of the torsional oscillation flow components (Jault & Le Mouël 1991; Jackson *et al.* 1993):

$$L_c^{(m)}(t) = \frac{I_c}{b}\left(t^{(m)0}_{\ 1} + \frac{12}{7}t^{(m)0}_{\ 3}\right). \tag{54}$$

The coefficients $t^{(m)0}_{\ 1}$ and $t^{(m)0}_{\ 3}$ are also measured with respect to the mantle fixed frame and are the coefficients obtained from the inversion of the geomagnetic data. Their relationship to the flow coefficients t_j^0 defined here with respect to a frame rotating at angular velocity Ω_o is given by

$$\begin{aligned} t_1^0 &= t^{(m)0}_{\ 1} + b\delta\Omega_m(t), \\ t_j^0 &= t^{(m)0}_{\ j}, \qquad \text{for } j > 1, \end{aligned} \tag{55}$$

where $\delta\Omega_m(t)$ is the change in mantle rotation rate with respect to Ω_o. In the reference frame rotating with angular velocity Ω_o, the total core angular momentum is then

$$\begin{aligned} L_c(t) &= L_c^{(m)}(t) + I_c\delta\Omega_m(t) \\ &= \frac{I_c}{b}\left(t^{(m)0}_{\ 1} + b\delta\Omega_m(t) + \frac{12}{7}t^{(m)0}_{\ 3}\right) \\ &= \frac{I_c}{b}\left(t_1^0 + \frac{12}{7}t_3^0\right). \end{aligned} \tag{56}$$

Conservation of angular momentum between the core and mantle implies that $L_c(t) = -L_m(t) = -I_m\delta\Omega_m(t)$, and by using $\delta\Omega_m = -\Delta T\Omega_o^2/2\pi$, from (56) we obtain a relationship between the torsional oscillation flow components and the changes in the length of day, namely

$$\left(t_1^0 + \frac{12}{7}t_3^0\right) = \frac{I_m}{I_c}\frac{\Omega_o^2 b}{2\pi}\Delta T. \tag{57}$$

The zonal harmonic degree 2 of the geostrophic forcing at the CMB in (38) contains the same ratio of t_1^0 to t_3^0,

$$\Psi_2^0(b) = -\frac{2}{3}\rho_o(b)\Omega_o b\left(t_1^0 + \frac{12}{7}t_3^0\right). \tag{58}$$

In other words, the zonal geostrophic pressure of harmonic degree 2 is directly proportional to the changes in length of day, and we can express $\Psi_2^0(b, t)$ directly in terms of ΔT by using (57). We note that this relationship should not be confused with the part of the pressure field that produces changes in length of day through topographic torques on the non-axisymmetric features at the CMB surface (Hide 1969, 1977; Jault & Le Mouël 1989).

Finally, the centrifugal potential in the mantle is related to the change in rotation rate of the mantle by $Z_2^{(m)} = 2\Omega_o\delta\Omega_m a^2/3$, and we can write the changes in J_2 in (52) as

$$\Delta J_2(t) = \frac{a^3\Omega_o^3}{3\pi GM}\Delta T\left(\frac{b^2}{a^2}\frac{\rho_o(b)}{\bar{\rho}}\frac{I_m}{I_c}k_2 - k_m\right). \tag{59}$$

We use a torsional oscillation flow model that is constrained to be consistent with the changes in the length of day. Our flow model is also constrained to give the best fit to the geomagnetic jerks (Bloxham *et al.* 2002), although this requirement does not affect the results presented below since only the variations in the length of day enter the changes in J_2. We show in Fig. 8 the first few coefficients of the torsional oscillation flow. Note that we have subtracted the mean steady component of each coefficient since we are interested in the changes with respect to a steady background. We show in Fig. 9 the data for length-of-day variations from the International Earth Rotation Service (IERS) and from which we have subtracted a secular change of 1.4 ms per century. We also show in the same figure the predicted changes from our torsional oscillation flow model. Our flow model serves as a smoothing and interpolating function for the observed changes in the length of day, and in all subsequent calculations the solid curve is used for ΔT.

One can extract from Fig. 9 the amplitude of $\Psi_n^0(b, t)$ produced by torsional oscillations by combining (57) and (58). The geostrophic pressure equivalent to a change in the length of day of 1 ms is roughly 40 Pa or 0.4 millibar.

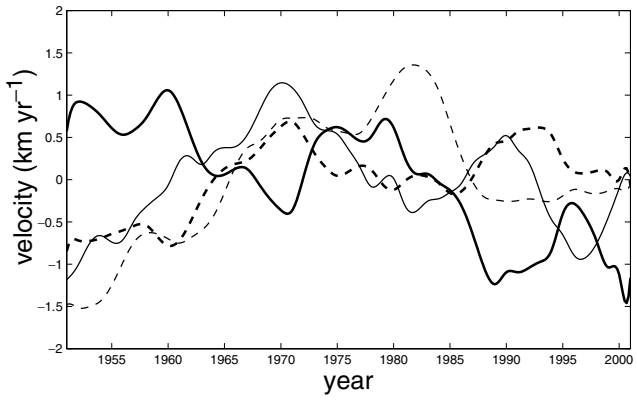

Figure 8. Coefficients of the torsional oscillation model as a function of time: t_1^0 (thick solid line); t_3^0 (thick dashed line); t_5^0 (thin solid line); t_7^0 (thin dashed line).

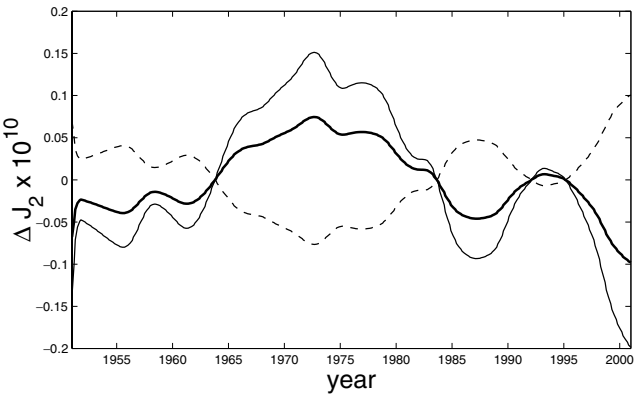

Figure 10. Variations in J_2 as a function of time predicted by our model (thick solid line), and its individual contributions from the k_2 term (thin solid line) and the k_m term (thin dashed line) of eq. (59).

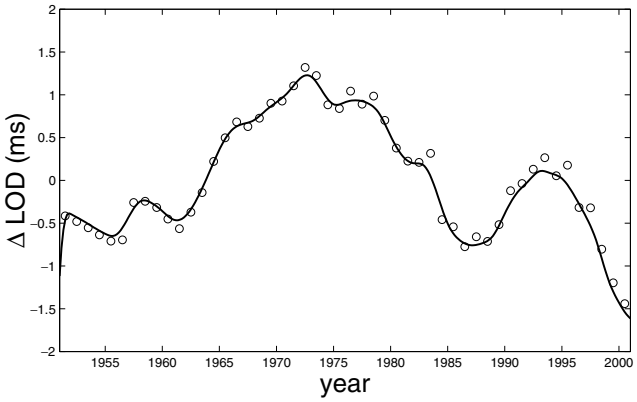

Figure 9. Variations in the length of day in milliseconds about an average value for the time period considered. The open circles are the data from the IERS, from which we have subtracted a trend of 1.4 milliseconds per century. The solid line is the prediction from the torsional oscillation flow model from eq. (57).

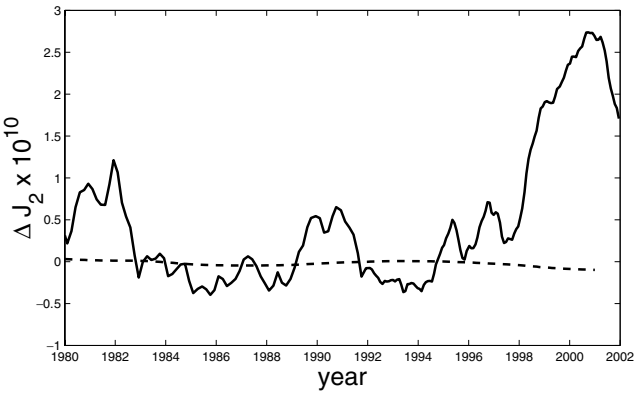

Figure 11. Comparison between the observed ΔJ_2 signal from which the secular linear trend has been removed (solid line) and variations in J_2 predicted by our model from eq. (59) (dashed line).

In Fig. 10 we show the changes in J_2 predicted by (59). The model predicts extrema in ΔJ_2 near the largest changes in the length of day, which is also when geomagnetic jerks are observed. This is because these are the times when the differential cylindrical velocities are the largest (Bloxham *et al.* 2002). The contribution from the change in rotation rate of the mantle is opposite to the contribution of the torsional oscillations, as expected, and is about a factor 2 smaller. The largest amplitude of the total variations in J_2 is roughly 2×10^{-11} for the last two decades. The largest rates of change in this time interval are roughly $\dot{J}_2 \sim 2 \times 10^{-12}$ yr^{-1}. The total variations in J_2 from our model are compared with the observed variations in J_2 about the secular linear trend for the last 20 yr in Fig. 11. Our model produces amplitudes that are too small by a factor of about 10 to explain the observed variations and by a factor of 30 to explain the larger variations that started near 1998. Moreover, the predicted changes in J_2 are not well correlated with the observations. This suggests that torsional oscillations in the core do not account for the subdecadal changes in J_2. Similarly, although we do not show it here, the changes in J_4 predicted by (51) are also a factor 10 too small and not well correlated with the observed changes in J_4 reported in Cox & Chao (2002).

As we see in Fig. 10, torsional oscillations also cause changes on longer timescales of about 30 yr. Since 1980, the overall variation in J_2 predicted from our torsional oscillation model is about -1.5×10^{-11}. This gives a mean rate of secular linear decrease of $\dot{J}_2 \sim -0.75 \times 10^{-12}$ yr^{-1}. This is about 40 times smaller than the observed linear trend of -2.8×10^{-11} yr^{-1} , which is believed to represent the signature of postglacial rebound (Yoder *et al.* 1983; Rubincam 1984; Mitrovica & Peltier 1993). However, this contribution from the torsional oscillations to the secular trend is of the same order as the effect produced by artificial reservoir water impoundment (Chao 1995), and more important than the effects produced by mass redistribution from earthquakes (Chao *et al.* 1995), subducting slabs in the mantle (Alfonsi & Spada 1998), and from the secular spin down and associated 'rounding' of the Earth due to gravitational tidal breaking with the Moon (e.g. Stacey 1992, p. 96).

The rates of change in J_2 predicted by our model, 10^{-12} to 2×10^{-12} yr^{-1}, are about an order of magnitude smaller than the value of 1.3×10^{-11} yr^{-1} reported by Fang *et al.* (1996). A difference of a factor 2 is due to the counter effect from the change in centrifugal potential of the mantle, which was not included in their model. Part of the remaining discrepancy is due to a difference in modelling. Fang *et al.* (1996) only solved the system of elastic-gravitational equations in the mantle with appropriate boundary conditions at the CMB and at the Earth's surface, and did not explicitly solve Poisson's equation in the core as we have done (Ming Fang, personal communication). In their model, the radial stress at the base of the mantle was prescribed to be exactly the applied geostrophic pressure

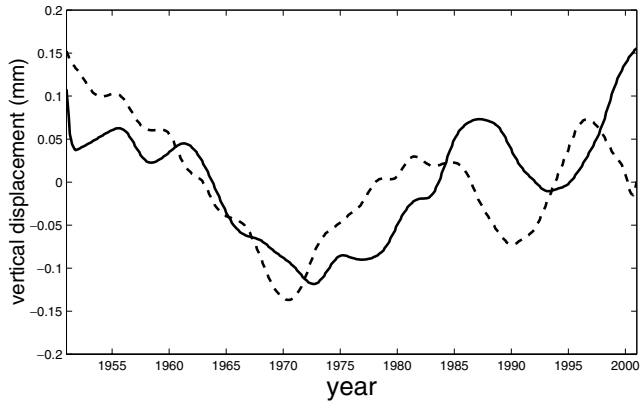

Figure 12. Variations in the zonal harmonic coefficients of degree 2 (solid line) and 4 (dashed line) of the vertical ground motion at the surface as a function of time.

(i.e. $y_2(b) = -\Psi_n^0$ in 41). We believe that this is incorrect as it does not take into account the adjustment in the radial stress that arises from the perturbation in the mechanical equilibrium. In fact, using their boundary condition on the radial stress in our model, we found that the value of k_2 increased from 0.116 to 0.190, a difference of almost a factor of 2. The remaining discrepancy between the result of this study and the study by Fang *et al.* (1996), a factor of 2 or 3, may be an additional consequence of solving Poisson's equation explicitly in the core. It may also be simply due to differences in the flow model. We note that the fact that they have used a general flow model as opposed to one strictly comprising torsional oscillations should produce no difference in J_2, as we demonstrate in Appendix B that only the torsional oscillation components of the flow produce zonal geostrophic pressure variations. However, a relatively small difference in the coefficients t_1^0 and t_3^0 of the flow model may easily produce a significant difference in the final result. This is because the changes in core angular momentum (which produce changes in length of day) result from small differences between the opposite individual contributions of t_1^0 and t_3^0 (see Fig. 8). Therefore, the remaining discrepancy between our result and that of Fang *et al.* (1996) may simply be a consequence of small differences in these two coefficients of the flow model.

Finally, we present in Fig. 12 the changes in the zonal harmonic coefficients of the radial displacement at the surface of the Earth, $\mathcal{D}_n(t)$, for degrees $n = 2$ and $n = 4$. They are obtained from the Love numbers defined in (50):

$$\begin{aligned} \mathcal{D}_2(t) &= \frac{1}{\bar{g}}\left(h_2 \frac{\Psi_n^0(b,t)}{\bar{\rho}} - h_{\rm m} Z_2^{(\rm m)}(t)\right), \\ \mathcal{D}_n(t) &= h_n \frac{\Psi_n^0(b,t)}{\bar{\rho}\bar{g}}, \qquad \text{for } n > 2, \end{aligned} \tag{60}$$

where we have again neglected the contribution from the change in inner core rotation rate. The changes in $\mathcal{D}_n(t)$ are of the order of 0.2 mm over the last few decades.

4 DISCUSSION AND CONCLUSION

The results of our study suggest that torsional oscillations in the core, in the simple way that they produce variable pressure at the CMB as we have described, cannot account for the observed changes in J_2 about the linear secular decreasing trend. The contribution to the linear secular trend itself that may be attributed to torsional oscillations is of the order of a few per cent. The correlation between geomagnetic jerks and the maxima in the changes in J_2, which was part of the motivation for this study, may, then, be merely a coincidence.

It is not impossible that torsional oscillations remain the underlying cause of the changes in J_2 about the linear trend if there exists an amplification mechanism. For instance, circulation in the oceans may amplify a 5-yr zonal degree 2 signal by a factor of 10, just as the tidal sea-level amplitudes near coast lines are greatly amplified (e.g. Gill 1982). However, because the prediction of our model and the observed signal are not well correlated, the amplification mechanism would have to be highly non-linear.

Even if the mechanism described in this study seems not to be responsible for the large sudden changes observed in J_2, the detection of torsional oscillations in the gravity data may be possible in the near future. If the source of the changes in J_2 is identified and subtracted from the signal, it may be possible to isolate a background global change in the degree 2 zonal harmonic. The results presented in this study suggest that the changes in J_2 from the torsional oscillations are of the order of 10^{-11} per decade, which is at the level of the present noise level in the gravity data (Cox & Chao 2002). However, the current GRACE satellite mission will provide data with a precision improvement of an order of magnitude (Kim & Tapley 2002; Chao 2003), and hence may allow the signal of the torsional oscillations to be observed in the changes in J_2. We stress, however, that the recovery of the torsional oscillation signal may not be possible if the time-varying parts of other effects that have similar amplitude cannot be eliminated from the data. Alternatively, the results of our model could be used to subtract the contribution from the torsional oscillations in the core in the time-varying part of the gravity field in order to isolate the changes due to other effects.

It may also be possible in the future to observe the vertical ground motion associated with torsional oscillations using global GPS data (e.g. Herring 1999). Our model predicts changes in vertical ground displacement at the surface of the order of 0.2 mm (Fig. 12). This is unfortunately below the current precision in measurements, which is a few millimetres. Perhaps with future improvements in the data, ground motion displacements could be used to observe torsional oscillations, although with the same caveats as for the gravity data. We note that the meridional displacements that our model predicts are an order of magnitude smaller than the vertical displacements and that there is little hope that they could be detected in the data.

The detection of torsional oscillations may be possible only in the lowest even harmonic degrees of the gravity field. As our results suggest, the gravity signal of torsional oscillations will be far below the level of detection for harmonic degrees larger than 4. Even for degree 4, it is unclear whether the torsional oscillations signal could be observed, even if one could remove the larger variations arising from other effects. Hence, the components of the torsional oscillation flow that may be observed with the gravity and ground motion data are probably restricted to t_1^0 and t_3^0. Observing these two components alone could, however, provide an invaluable check of consistency for the modelling of core angular momentum.

Because of the possibility that future gravity data might provide sufficient accuracy for identifying the low harmonic signal from torsional oscillations, we may want to include additional refinements in our model. One improvement is to add a surface ocean. The solid surface only adjusts partly to the imposed gravitational potential because of its elastic rigidity. The surface of the ocean, on the other hand, would deform exactly to the imposed potential. Hence, an additional radial mass displacement would occur and contribute to an additional change in potential. It is difficult to predict exactly

the change in gravitational potential that would arise without doing the actual calculations. We note, however, that the density of water in the ocean is three times smaller than that of the crust and only represents a tiny fraction of the Earth's radius. Therefore, the oceans would probably not contribute to large changes in the gravitational potential. By incorporating a surface ocean in our model, however, we should be able to predict the time variations in the even harmonic degrees of the sea level around the globe. These could be then be compared with altimetry data.

One possible additional refinement to our model is the incorporation of viscous dissipation in the mantle and inner core. We are currently defining the mantle and inner core to be perfectly elastic, but if we allow for anelastic effects, the amplitude of the perturbations may be altered and delayed. Using a realistic viscoelastic rheology for the mantle and inner core with a viscosity profile akin to that used in postglacial rebound studies (Peltier 1974; Wu & Peltier 1982) would probably not alter our results significantly. This is because the forcing of torsional oscillations acts at decadal periods, which is much shorter than the typical timescale of a thousand years on which the viscous relaxation is observed to occur. However, if there exists a layer with a smaller viscosity at the bottom of the mantle, then perhaps the anelastic effects on the gravity signal from the torsional oscillations may be important, if not in amplitude then in delaying the observed signal. Such a low-viscosity layer at the base of the mantle is hinted at by seismological observations of ultra-low-velocity zones (Wen & Helmberger 1998; Garnero *et al.* 1998). Therefore, the mechanism that we have presented in this study may in the future provide a useful tool for testing geodynamically the nature of these seismological observations.

ACKNOWLEDGMENTS

The authors wish to thank Chris Cox for providing the data for J_2, Bruce Buffett for an initial version of the numerical code used in this study, and Ming Fang for discussions about the details of the model used in Fang *et al.* (1996). We are also indebted to Richard Holme for a thorough review, which improved this paper significantly. MD is partially funded by NSERC/CRSNG and FCAR scholarships. This work was also supported by NSF Awards EAR-0073988 and EAR-0327843.

REFERENCES

Alfonsi, L. & Spada, G., 1998. Effect of subductions and trends in seismically induced Earth rotational variations, *J. geophys. Res.,* **103,** 7351–7362.

Alterman, Z., Jarosch, H. & Pekeris, C.L., 1959. Oscillations of the Earth, *Proc. R. Soc. Lond.,* A, **252,** 80–95.

Bloxham, J. & Jackson, A., 1991. Fluid flow near the surface of Earth's outer core, *Rev. Geophys.,* **29,** 97–120.

Bloxham, J., Zatman, S. & Dumberry, M., 2002. The origin of geomagnetic jerks, *Nature,* **420,** 65–68.

Braginsky, S.I., 1970. Torsional magnetohydrodynamic vibrations in the Earth's core and variations in day length, *Geomag. Aeron.,* **10,** 1–10.

Braginsky, S.I., 1984. Short-period geomagnetic secular variation, *Geophys. astrophys. Fluid Dyn.,* **30,** 1–78.

Buffett, B.A., 1996. Gravitational oscillations in the length of the day, *Geophys. Res. Lett.,* **23,** 2279–2282.

Buffett, B.A., 1998. Free oscillations in the length of day: inferences on physical properties near the core–mantle boundary, in *The Core–Mantle Boundary Region,* Vol. 28, pp. 153–165, eds Gurnis, M., Wysession, M.E., Knittle, E. & Buffett, B.A., Geodynamics series, AGU Geophysical Monograph, Washington, DC.

Bullard, E.C. & Gellman, H., 1954. Homogeneous dynamos and terrestrial magnetism, *Phil. Trans. R. Soc. Lond.,* A, **247,** 213–278.

Chao, B.F., 1995. Anthropogenic impact on global geodynamics due to reservoir water impoundment, *Geophys. Res. Lett.,* **22,** 3529–3532.

Chao, B.F., 2003. Geodesy is not just for static measurements any more, *EOS, Trans. Am. geophys. Un.,* **84,** 145.

Chao, B.F., Gross, R.S. & Dong, D.N., 1995. Changes in the global gravitational energy induced by earthquakes, *Geophys. J. Int.,* **122,** 784–789.

Chao, B.F., Au, A.Y., Boy, J.-P. & Cox, C.M., 2003. Time-variable gravity signal of an anomalous redistribution of water mass in the extratropic Pacific during 1998–2002, *Geochem. Geophys. Geosyst.,* **4,** 1096, doi:10.1029/2003GC000589.

Chinnery, M.A., 1975. The static deformation of an Earth with a fluid core: a physical approach, *Geophys. J. R. astr. Soc.,* **42,** 461–475.

Cox, C.M. & Chao, B.F., 2002. Detection of large-scale mass redistribution in the terrestrial system since 1998, *Science,* **297,** 831–833.

Crossley, D.J., 1975. The free oscillation equations at the center of the Earth, *Geophys. J. R. astr. Soc.,* **41,** 153–163.

Crossley, D.J. & Gubbins, D., 1975. Static deformation of the Earth's liquid core, *Geophys. Res. Lett.,* **2,** 1–4.

Dahlen, F.A., 1972. Elastic dislocation theory for a self-gravitating elastic configuration with an initial static stress field, *Geophys. J. R. astr. Soc.,* **28,** 357–383.

Dahlen, F.A., 1974. On the static deformation of an Earth model with a fluid core, *Geophys. J. R. astr. Soc.,* **36,** 461–485.

Dahlen, F.A. & Fels, S.B., 1978. A physical explanation for the static core paradox, *Geophys. J. R. astr. Soc.,* **55,** 317–332.

Dahlen, F.A. & Trump, J., 1998. *Theoretical Global Seismology,* Princeton University Press, Princeton, NJ.

Denis, C., Almavict, M., Rogister, Y. & Tomecka-Suchon, S., 1998. Methods for computing internal flattening, with applications to the Earth's structure and geodynamics, *Geophys. J. Int.,* **132,** 603–642.

Dickey, J.O., Marcus, S.L., de Viron, O. & Fukumori, I., 2002. Recent Earth oblateness variations: unraveling climate and postglacial rebound effects, *Science,* **298,** 1975–1977.

Dumberry, M. & Bloxham, J., 2003. Torque balance, Taylor's constraint and torsional oscillations in a numerical model of the geodynamo, *Phys. Earth planet. Inter.,* **140,** 29–51.

Dziewonski, A.M. & Anderson, D.L., 1981. Preliminary reference Earth model, *Phys. Earth planet. Inter.,* **25,** 297–356.

Fang, M., 1998. Static deformation of the outer core, in *Dynamics of the Ice Age Earth: A Modern Perspective,* Vols 3–4, pp. 155–190, ed. Wu, P., GeoResearch Forum, Trans Tech Publications, Zürich, Switzerland.

Fang, M., Hager, B.H. & Herring, T.A., 1996. Surface deformation caused by pressure changes in the fluid core, *Geophys. Res. Lett.,* **23,** 1493–1496.

Garnero, E.J., Ravenaugh, J., Williams, Q., Lay, T. & Kellogg, L.H., 1998. Ultralow velocity zone at the core–mantle boundary, in *The Core–Mantle Boundary Region,* Vol. 28, pp. 319–334, eds Gurnis, M., Wysession, M.E., Knittle, E. & Buffett, B.A., Geodynamics series, AGU Geophysical Monograph, Washington, DC.

Gavoret, J., Gilbert, D., Menvielle, M. & LeMouël, J.-L., 1986. Long-term variations of the external and internal components of the Earth's magnetic field, *J. geophys. Res.,* **91,** 4787–4796.

Gill, A.E., 1982. *Atmosphere–Ocean Dynamics,* Vol. 30, International geophysics series, Academic Press, London.

Gire, C. & Le Mouël, J.-L., 1990. Tangentially geostrophic flow at the core–mantle boundary compatible with the observed geomagnetic secular variation: the large-scale component of the flow, *Phys. Earth planet. Inter.,* **59,** 259–287.

Gubbins, D., 1981. Rotation of the inner core, *J. geophys. Res.,* **86,** 11 695–11 699.

Gubbins, D. & Tomlinson, L., 1986. Secular variations from monthly means from Apia and Amberley magnetic observatories, *Geophys. J. R. astr. Soc.,* **86,** 603–616.

Herring, T.A., 1999. Geodetic applications of GPS, *Proc. IEEE,* **87,** 92–110.

Hide, R., 1969. Interaction between the Earth's liquid core and solid mantle, *Nature,* **222,** 1055–1056.

Hide, R., 1977. Towards a theory of irregular variations in length of day and core–mantle coupling, *Phil. Trans. R. Soc. Lond.,* A, **284,** 547–554.
Hide, R., Boggs, D.H. & Dickey, J.O., 2000. Angular momentum fluctuations within the Earth's liquid core and torsional oscillations of the core–mantle system, *Geophys. J. Int.,* **143,** 777–786.
Hills, R.G., 1979. Convection in the Earth's mantle due to viscous shear at the core–mantle interface and due to large-scale buoyancy, *PhD thesis,* New Mexico State University, Las Cruces.
Israel, M., Ben-Manahem, A. & Singh, S.J., 1973. Residual deformation of real Earth models with application to the Chandler wobble, *Geophys. J. R. astr. Soc.,* **32,** 219–247.
Jackson, A., Bloxham, J. & Gubbins, D., 1993. Time-dependent flow at the core surface and conservation of angular momentum in the coupled core–mantle system, in *Dynamics of the Earth's Deep Interior and Earth Rotation,* Vol. 72, pp. 97–107, eds Le Mouël, J.-L., Smylie, D.E. & Herring, T., AGU Geophysical Monograph, Washington, DC.
Jault, D. & Le Mouël, J.-L., 1989. The topographic torque associated with a tangentially geostrophic motion at the core surface and inferences on the flow inside the core, *Geophys. astrophys. Fluid Dyn.,* **48,** 273–296.
Jault, D. & Le Mouël, J.-L., 1991. Exchange of angular momentum between the core and the mantle, *J. Geomag. Geoelectr.,* **43,** 111–129.
Jault, D., Gire, C. & Le Mouël, J.-L., 1988. Westward drift, core motions and exchanges of angular momentum between core and mantle, *Nature,* **333,** 353–356.
Jeffreys, H., 1970. *The Earth,* 5th edn, Cambridge University Press, London.
Jeffreys, H. & Vicente, R.O., 1966. Comparisons of forms of the elastic equations for the Earth, *Mem. Acad. R. Belgique,* **37,** 5–31.
Kim, J. & Tapley, B.D., 2002. Error analysis of a low-low satellite-to-satellite tracking mission, *J. Guid. control Dynam.,* **25,** 1100–1106.
Laske, G. & Masters, G., 1999. Limits on differential rotation of the inner core from an analysis of the Earth's free oscillations, *Nature,* **402,** 66–69.
Le Mouël, J.-L., 1984. Outer core geostrophic flow and secular variation of Earth's magnetic field, *Nature,* **311,** 734–735.
Lefftz, M. & Legros, H., 1992. Influence of viscoelastic coupling on the axial rotation of the earth and its fluid core, *Geophys. J. Int.,* **108,** 725–739.
Longman, I.M., 1963. A green's function for determining the deformation of the Earth under surface mass loads: 2. Computations and numerical results, *J. geophys. Res.,* **68,** 485–496.
Love, A.E.H., 1909. The yielding of the Earth to disturbing forces, *Proc. R. Soc. Lond.,* A, **82,** 73–88.
Macmillan, S., 1996. A geomagnetic jerk for the early 1990's, *Earth planet. Sci. Lett.,* **137,** 189–192.
Mandea, M., Bellanger, E. & LeMouël, J.-L., 2000. A geomagnetic jerk for the end of the 20th century?, *Earth planet. Sci. Lett.,* **183,** 369–373.
Mitrovica, J.X. & Peltier, W.R., 1993. Present-day variations in the zonal harmonics of the Earth's geopotential, *J. geophys. Res.,* **98,** 4509–4526.
Mound, J.E. & Buffett, B.A., 2003. Interannual oscillations in the length of day: implications for the structure of mantle and core, *J. geophys. Res.,* **108**(B7), 2334, doi:10.1029/2002JB002054.
Munk, W.H. & MacDonald, G. J.F., 1960. *The Rotation of the Earth,* Cambridge University Press, Cambridge.
Pais, A. & Hulot, G., 2000. Length of day decade variations, torsional oscillations and inner core superrotation: evidence from recovered core surface zonal flows, *Phys. Earth planet. Inter.,* **118,** 291–316.
Pekeris, C.L. & Accad, Y., 1972. Dynamics of the liquid core of the Earth, *Phil. Trans. R. Soc. Lond.,* A, **273,** 237–260.
Peltier, W.R., 1974. The impulse response of a Maxwell Earth, *Rev. Geophys.,* **12**, 649–669.
Rubincam, D.P., 1984. Postglacial rebound observed by LAGEOS and the effective viscosity of the lower mantle, *J. geophys. Res.,* **89,** 1077–1087.
Smylie, D.E. & Mansinha, L., 1971. The elastic theory of dislocation in real Earth models and changes in the rotation of the Earth, *Geophys. J. R. astr. Soc.,* **23,** 329–354.
Song, X.D. & Richards, P.G., 1996. Seismological evidence for differential rotation of the Earth's inner core, *Nature,* **382,** 221–224.
Souriau, A. & Poupinet, G., 2000. Inner core rotation: a test at the worldwide scale, *Phys. Earth planet. Inter.,* **118,** 13–27.
Stacey, F.D., 1992. *Physics of the Earth,* 3rd edn, Brookfield Press, Kenmore, Australia.
Su, W.J., Dziewonski, A.M. & Jeanloz, R., 1996. Planet within a planet: Rotation of the inner core of the Earth, *Science,* **274,** 1883–1887.
Takeushi, H. & Saito, M., 1972. Seismic surface waves, in *Methods of Computational Physics,* Vol. 11, pp. 217–295, ed. Bolt, B.A., Academic Press, San Diego.
Taylor, J.B., 1963. The magneto-hydrodynamics of a rotating fluid and the Earth's dynamo problem, *Proc. R. Soc. Lond.,* A, **274,** 274–283.
Wen, L.X. & Helmberger, D.V., 1998. Ultra-low velocity zones near the core–mantle boundary from broadband PKP precursors, *Science,* **279,** 1701–1703.
Wu, P. & Peltier, D.R., 1982. Viscous gravitational relaxation, *Geophys. J. R. astr. Soc.,* **70,** 435–485.
Yoder, C.F., Williams, J.G., Dickey, J.O., Schutz, B.E., Eanes, R.J. & Tapley, B.D., 1983. Secular variation of the Earth's gravitational harmonic j_2 coefficient from LAGEOS and nontidal acceleration of Earth rotation, *Nature,* **303,** 757–762.
Zatman, S., 2003. Decadal oscillations of the Earth's core, angular momentum exchange, and inner core rotation, in *Earth's Core: Dynamics, Structure, Rotation,* Vol. 31, pp. 233–240, eds Dehant, V., Creager, K.C., Karato, S.-I. & Zatman, S., Geodynamics series, AGU Geophysical Monograph, Washington, DC.
Zatman, S. & Bloxham, J., 1997. Torsional oscillations and the magnetic field within the Earth's core, *Nature,* **388,** 760–763.
Zatman, S. & Bloxham, J., 1998. A one-dimensional map of B_s from torsional oscillations of the Earth's core, in *The Core–Mantle Boundary Region,* Vol. 28, pp. 183–196, eds Gurnis, M., Wysession, M.E., Knittle, E. & Buffett, B.A., Geodynamics series, AGU Geophysical Monograph, Washington, DC.
Zatman, S. & Bloxham, J., 1999. On the dynamical implications of models of B_s in the Earth's core, *Geophys. J. Int.,* **138,** 679–686.

APPENDIX A: ELASTIC-GRAVITATIONAL EQUATIONS IN THE SOLID EARTH

The static elastic-gravitational equations in the mantle in terms of the six variables defined in (15) have to obey the differential equations

$$\frac{\partial y_1}{\partial r} = \frac{1}{\lambda_o + 2\mu_o}\left(y_2 - \frac{\lambda_o}{r}(2y_1 - n(n+1)y_3)\right),$$

$$\frac{\partial y_2}{\partial r} = \frac{2}{r}\left(\lambda_o \frac{\partial y_1}{\partial r} - y_2\right) + \left(\frac{2(\lambda_o + \mu_o)}{r} - \rho_o g_o\right)\left(2y_1 - \frac{n(n+1)}{r}y_3\right) + \frac{n(n+1)}{r}y_4 + \rho_o\left(y_6 - \frac{n+1}{r}y_5 - 2\frac{g_o}{r}y_1\right),$$

$$\frac{\partial y_3}{\partial r} = \frac{1}{\mu_o}y_4 + \frac{1}{r}(y_3 - y_1),$$

$$\frac{\partial y_4}{\partial r} = -\frac{\lambda_o}{r}\frac{\partial y_1}{\partial r} - \left(\frac{\lambda_o + 2\mu_o}{r^2}(2y_1 - n(n+1)y_3) - \frac{2\mu_o}{r^2}(y_1 - y_3)\right) - \frac{3}{r}y_4 + \frac{\rho_o}{r}(y_5 + g_o y_1),$$

$$\frac{\partial y_5}{\partial r} = y_6 - 4\pi G\rho_o y_1 - \frac{n+1}{r} y_5,$$
$$\frac{\partial y_6}{\partial r} = \frac{n-1}{r} y_6 - 4\pi G\rho_o \frac{n+1}{r} y_1 + 4\pi G\rho_o \frac{n(n+1)}{r} y_3. \tag{A1}$$

We note that the equations above are identical to those in Takeushi & Saito (1972) for zero frequency, except that y_5 and y_6 have opposite signs as a consequence of a different sign convention adopted in the present study. The equations in the inner core are identical.

APPENDIX B: CALCULATION OF GEOSTROPHIC PRESSURE FROM CORE SURFACE FLOWS

In this Appendix, we present the details of the calculation relating the even-degree zonal harmonics of the pressure at the CMB to torsional oscillations. We demonstrate that, for a general flow at the CMB, torsional oscillations are in fact the only component of the flow that participate in the axisymmetric pressure that is symmetric about the equator.

Near the CMB, the horizontal component of the flow is related to pressure through the geostrophic balance (Hills 1979; Le Mouël 1984):

$$2\rho_o \mathbf{\Omega} \times \mathbf{v_h} = -\boldsymbol{\nabla} p_g. \tag{B1}$$

Taking $\mathbf{e_r}\times$ (B1) and using $\mathbf{e}_r \times \mathbf{e}_z \times \mathbf{v}_h = -\cos\theta\, \mathbf{v}_h$, we have

$$2\Omega_o b\rho_o \cos\theta \mathbf{v_h} = \mathbf{e_r} \times \boldsymbol{\nabla}_1 p_g, \tag{B2}$$

where b is the radius of the core and $\boldsymbol{\nabla}_1$ is defined in (11). The geostrophic pressure is expanded in spherical harmonics according to (37), and we want to relate the coefficients of the latter in terms of core surface flows. It is convenient to expand $\mathbf{v_h}$ in a poloidal–toroidal decomposition, namely

$$\mathbf{v_h} = \boldsymbol{\nabla}_1 \mathcal{S} + \boldsymbol{\nabla}_1 \times (\mathcal{T}\mathbf{e_r}) = \boldsymbol{\nabla}_1 \mathcal{S} - \mathbf{e_r} \times \boldsymbol{\nabla}_1 \mathcal{T}, \tag{B3}$$

where $\mathcal{S}$ and $\mathcal{T}$ are respectively the poloidal and toroidal scalars. The latter are expanded in spherical harmonics as

$$\mathcal{S} = \sum_{n=0}^{\infty} \sum_{m=-n}^{n} s_n^m Y_n^m, \tag{B4}$$

$$\mathcal{T} = \sum_{n=0}^{\infty} \sum_{m=-n}^{n} t_n^m Y_n^m. \tag{B5}$$

We note that the custom in geomagnetism is to use a decomposition in terms of real spherical harmonics. However, it is convenient here to expand the flow coefficients as above so as to be consistent with our expansion of pressure.

In order to relate the flow coefficients s_n^m and t_n^m to the coefficients of pressure $\Psi_n^m(b)$, we use the vector spherical harmonics $\mathbf{B}_n^m = \mathbf{B}_n^m(\theta, \varphi)$ and $\mathbf{C}_n^m = \mathbf{C}_n^m(\theta, \varphi)$, which are related to the spherical harmonic scalar $Y_n^m = Y_n^m(\theta, \varphi)$ by

$$\mathbf{B}_n^m = \boldsymbol{\nabla}_1 Y_n^m = \mathbf{e}_\theta \frac{\partial}{\partial\theta} Y_n^m + \mathbf{e}_\varphi \frac{1}{\sin\theta} \frac{\partial}{\partial\varphi} Y_n^m, \tag{B6}$$

$$\mathbf{C}_n^m = \mathbf{e_r} \times \boldsymbol{\nabla}_1 Y_n^m = \mathbf{e}_\varphi \frac{\partial}{\partial\theta} Y_n^m - \mathbf{e}_\theta \frac{1}{\sin\theta} \frac{\partial}{\partial\varphi} Y_n^m. \tag{B7}$$

Using these definitions, we can write (B2) as

$$2\Omega_o b\rho_o \cos\theta \sum_{n'=0}^{\infty} \sum_{m'=-n'}^{n'} \left(s_{n'}^{m'} \mathbf{B}_{n'}^{m'} - t_{n'}^{m'} \mathbf{C}_{n'}^{m'} \right) = \sum_{n=0}^{\infty} \sum_{m=-n}^{n} \Psi_n^m(b)\, \mathbf{C}_n^m. \tag{B8}$$

The coefficients $\Psi_n^m(b)$ are obtained by projecting the above equation on the basis $\mathbf{C}_n^{m*}$ and integrating over the surface of the unit sphere. Using the orthogonality rules on the spherical harmonics and the normalization defined in (13), we obtain, for each n and m,

$$\Psi_n^m(b) = \frac{2\Omega_o b\rho_o}{4\pi} \frac{2n+1}{n(n+1)} \sum_{n'=0}^{\infty} \sum_{m'=-n'}^{n'} \left(s_{n'}^{m'} \int_\Omega \mathbf{C}_n^{m*} \cdot \mathbf{B}_{n'}^{m'} \cos\theta\, d\Omega - t_{n'}^{m'} \int_\Omega \mathbf{C}_n^{m*} \cdot \mathbf{C}_{n'}^{m'} \cos\theta\, d\Omega \right). \tag{B9}$$

The role of each flow coefficient in the pressure depends on an integral of spherical harmonics over a sphere. To solve these integrals, one possibility is to use the fact that $\cos\theta = P_1^0(\cos\theta) = Y_1^0$. We then have integrals of triple products of spherical harmonics, which are non-zero for a set of conditions on the indices (see for instance Bullard & Gellman 1954 or Dahlen & Trump 1998). For the even-degree zonal coefficients of the geostrophic pressure, $\Psi_n^0(b)$ with n= *even*, the selection rules are such that the poloidal integral (the $s_{n'}^{m'}$ term) vanishes for all indices. The toroidal integral (the $t_{n'}^{m'}$ term) is non-zero only for $m' = 0$, and the only components of the flow that contribute are the $t_{n'}^0$ with $n' = odd$.

However, a perhaps more transparent way to demonstrate this, and also to solve these integrals, is instead simply to expand the above integrals using the definitions in (B6–B7). The poloidal integral is

$$\int_\Omega \mathbf{C}_n^{m*} \cdot \mathbf{B}_{n'}^{m'} \cos\theta \, d\Omega = \int_\Omega \left(\frac{\partial Y_n^{m*}}{\partial \theta} \frac{\partial Y_{n'}^{m'}}{\partial \varphi} - \frac{\partial Y_n^{m*}}{\partial \varphi} \frac{\partial Y_{n'}^{m'}}{\partial \theta} \right) \frac{\cos\theta}{\sin\theta} \, d\Omega$$
$$= -\int_\Omega \frac{\cos\theta}{\sin\theta} \frac{\partial}{\partial \theta} \left(Y_{n'}^{m'} \frac{\partial Y_n^{m*}}{\partial \varphi} \right) d\Omega. \tag{B10}$$

Further algebraic efforts are needed in order to solve the integral for a general set of indices. However, for the zonal coefficients of pressure ($m = 0$), $\partial Y_n^0/\partial\varphi = 0$ and the integral vanishes for all values of n, n' and m'. Hence, the poloidal flow components do not contribute to the axisymmetric pressure at the CMB. This simply illustrates the well-known fact the axisymmetric part of tangential geostrophy can only be explained in terms of toroidal flows.

The toroidal integral, for $m = 0$, is

$$\int_\Omega \mathbf{C}_n^{0*} \cdot \mathbf{C}_{n'}^{m'} \cos\theta \, d\Omega = \int_\Omega \left(\frac{\partial Y_n^0}{\partial \theta} \frac{\partial Y_{n'}^{m'}}{\partial \theta} \right) \cos\theta \, d\Omega$$
$$= \int_\Omega \left(\frac{\partial P_n^0}{\partial \theta} \frac{\partial Y_{n'}^{m'}}{\partial \theta} \right) \cos\theta \, d\Omega. \tag{B11}$$

The right-hand side can be further decomposed as

$$\int_\Omega \mathbf{C}_n^{0*} \cdot \mathbf{C}_{n'}^{m'} \cos\theta \, d\Omega = \int_\Omega Y_{n'}^{m'} \sin\theta \frac{\partial P_n^0}{\partial \theta} \, d\Omega - \int_\Omega Y_{n'}^{m'} \frac{\cos\theta}{\sin\theta} \frac{\partial}{\partial \theta} \sin\theta \frac{\partial P_n^0}{\partial \theta} \, d\Omega. \tag{B12}$$

Using

$$-\frac{1}{\sin\theta} \frac{\partial}{\partial \theta} \sin\theta \frac{\partial P_n^0}{\partial \theta} = L^2 P_n^0 = n(n+1) P_n^0, \tag{B13}$$

we can write (B12) as

$$\int_\Omega \mathbf{C}_n^{0*} \cdot \mathbf{C}_{n'}^{m'} \cos\theta \, d\Omega = \int_\Omega Y_{n'}^{m'} \sin\theta \frac{\partial P_n^0}{\partial \theta} \, d\Omega + n(n+1) \int_\Omega Y_{n'}^{m'} \cos\theta P_n^0 \, d\Omega. \tag{B14}$$

The above integrals can be transformed into simple orthogonality integrals of spherical harmonics with the use of the following recurrence relations for the associated Legendre polynomials,

$$\sin\theta \frac{\partial P_n^0}{\partial \theta} = -\frac{n(n+1)}{2n+1} P_{n-1}^0 + \frac{n(n+1)}{2n+1} P_{n+1}^0, \tag{B15}$$

$$\cos\theta P_n^0 = \frac{n}{2n+1} P_{n-1}^0 + \frac{n+1}{2n+1} P_{n+1}^0. \tag{B16}$$

Eq. (B14) then becomes

$$\int_\Omega \mathbf{C}_n^{0*} \cdot \mathbf{C}_{n'}^{m'} \cos\theta \, d\Omega = \frac{n(n+1)}{2n+1} \left((n-1) \int_\Omega Y_{n'}^{m'} P_{n-1}^0 \, d\Omega + (n+2) \int_\Omega Y_{n'}^{m'} P_{n+1}^0 \, d\Omega \right)$$
$$= 4\pi \frac{n(n+1)}{2n+1} \left(\frac{n-1}{2n-1} \delta_{n'(n-1)} \delta_{m'0} + \frac{n+2}{2n+3} \delta_{n'(n+1)} \delta_{m'0} \right) \tag{B17}$$

For a given harmonic degree n, the only non-zero integrals are therefore those with $m' = 0$, and n' equal to either $(n-1)$ or $(n+1)$. Hence, only the axisymmetric components of the toroidal flow participate in the zonal geostrophic pressure, and for each zonal harmonic degree of the latter, only two of the zonal toroidal flow coefficients contribute. Moreover, for a geostrophic pressure symmetric about the equator ($n = even$), only the flow coefficients with *odd* harmonic degree participate. In other words, the only flow components that participate in the even-degree zonal harmonics of the pressure are torsional oscillations. The final expression for the zonal harmonic degree n of the geostrophic pressure at the CMB is obtained by substituting (B17) into (B9):

$$\Psi_n^0(b) = -\Omega_o b \rho_o \left(\frac{2(n-1)}{(2n-1)} t_{n-1}^0 + \frac{2(n+2)}{(2n+3)} t_{n+1}^0 \right). \tag{B18}$$

APPENDIX C: ANALYTICAL SOLUTION OF THE ELASTIC-GRAVITATIONAL EQUATIONS NEAR THE ORIGIN

The solution in the inner core near the centre of the Earth is detailed in the study of Crossley (1975). At a small radius $r = \epsilon$, the solution can be written in terms of three independent solutions. A convenient way to write the complete solution is in terms of three vectors, $\mathbf{y}^{\epsilon 1}$, $\mathbf{y}^{\epsilon 2}$ and $\mathbf{y}^{\epsilon 3}$, as

$$\mathbf{y}^s(\epsilon) = C_1 \mathbf{y}^{\epsilon 1} + C_2 \mathbf{y}^{\epsilon 2} + C_3 \mathbf{y}^{\epsilon 3}, \tag{C1}$$

where

$$\mathbf{y}^{\epsilon\mathbf{1}} = \left[\epsilon^{n-1}, 2(n-1)\mu_o\epsilon^{n-2}, \frac{\epsilon^{n-1}}{n}, \frac{2(n-1)}{n}\mu_o\epsilon^{n-2}, -\frac{3\gamma}{2n+1}\epsilon^n, 0\right]^{\mathrm{T}},$$

$$\mathbf{y}^{\epsilon\mathbf{2}} = \left[0, 0, 0, 0, \frac{\epsilon^n}{(2n+1)}, \epsilon^{n-1}\right]^{\mathrm{T}},$$

$$\mathbf{y}^{\epsilon\mathbf{3}} = \left[\alpha_1\epsilon^{n+1}, \alpha_2\epsilon^n, \alpha_3\epsilon^{n+1}, \epsilon^n, \alpha_5\epsilon^{n+2}, \alpha_6\epsilon^{n+1}\right]^{\mathrm{T}}, \tag{C2}$$

with

$$\alpha_3 = \frac{p_2}{p_1} - \frac{\rho_o}{C_3 p_1}\left(C_1\gamma n\left(1 - \frac{3}{2n+1}\right) + C_2\frac{n}{2n+1}\right),$$

$$\alpha_1 = -n\alpha_3 + \frac{1}{\mu_o},$$

$$\alpha_2 = -q_1\alpha_3 + q_2,$$

$$\alpha_5 = \frac{3\gamma}{2(2n+3)}\left(-(n+3)\alpha_1 + n(n+1)\alpha_3\right),$$

$$\alpha_6 = 3\gamma\alpha_1 + (2n+3)\alpha_5, \tag{C3}$$

and

$$\gamma = \frac{4\pi}{3}G\rho_o$$

$$p_1 = 2n^2(n+2)\lambda_o + 2n(n^2+2n-1)\mu_o,$$

$$p_2 = n(n+5) + 2n(n+3)\frac{\lambda_o}{\mu_o},$$

$$q_1 = 2n(n+2)\lambda_o + 2n(n+1)\mu_o,$$

$$q_2 = 2(n+1) + (n+3)\frac{\lambda_o}{\mu_o}. \tag{C4}$$

In the above equations, ρ_o, λ_o and μ_o correspond to the reference-state values evaluated at $r = \epsilon$. We note that the small differences between the analytical solution presented above and that of Crossley (1975) are a result of the different definitions of y_5^s and y_6^s used in the present study.